UNIVERSITY OF OVIEDO

Analysis of spatiotemporal Patterns of oceanographic variables obtained from Remote Sensing:

Spatio-temporal pattern of Sea Surface Temperature in Northern Iberia Shelf.

Author: Henok Mulugeta Debalkie

External Advisor: Rafael González- Quirós

Internal Advisor: Carmen Recondo González

July, 2014

ACKNOWLEDGMENTS

Table of Contents

List of Figures

List of Acronyms

AVHRR	Advanced Very High Resolution Radiometer
c.	circa
EOF	Empirical Orthogonal Function
ENACWT	Eastern North Atlantic Central Water of sub-tropical origin
ERDDAP	Environmental Research Division's Data Access Program
IPC	Iberian Poleward Current
MODIS	Moderate Resolution Imaging Spectroradiometer
NASA	National Aeronautics and Space Administration
NetCDF	Network Common Data Form
NIS	Northern Iberia Shelf
NLSST	Non-Linear Sea Surface Temperature
NOAA	National Oceanic and Atmospheric Administration
PC	Principal Component
POES	Polar Operational Environmental Satellite
SEA	Southeastern European Atlantic
SPCA	Standardized Principle Component Analysis
SST	Sea Surface Temperature

Abstract

A time series analysis of Sea Surface Temperature (SST) data derived from the NOAA/NASA Advanced Very High Resolution Radiometer (AVHRR) Pathfinder V5 and MODIS (Moderate Resolution Imaging Spectroradiometer) Aqua data over the Northern Iberia Shelf (NIS) covering the period 1982-2012 was analyzed with Empirical Orthogonal Function (EOF) in order to define the spatial pattern, timing and relative magnitude of seasonal and interannual variability of SST. For the NIS, Principal Component number 1(PC1) accounted for more than 90% of the variability. The loadings showed a strong seasonal cyclic signal and the spatial scores a conspicuous gradient across the area of study. The combination of the pattern of the loadings and the scores reflected spatial differences in the amplitude of the SST seasonal signal. The strong seasonal signal was also observed at a larger scale in the Southeastern European Atlantic (SEA). The analysis of the spatial pattern in the Northern Iberian Shelf (NIS) indicated that SST during summer time at the western Iberian Shelf was lower and it increased along the Cantabrian shelf, becoming maximum at the inner Bay of Biscay. However, this process was reversed in winter, when temperature was maximum at the western Iberian shelf and it decreased towards the Cantabrian shelf and being minimum at the inner Bay of Biscay. This indicates that there existed a strong spatial and temporal variation of SST in the study area. The comparison between the NIS and the SEA allowed hypothesizing about the nature of the processes that may govern interannual variability in the NIS; i.e. similar variability in both areas could corresponded to large scale forcing processes, whereas differences between NIS and SEA could be indicative of the relative importance mesoscale processes in the NIS. The influence that the main mesoscale processes (i.e., coastal upwelling, the Iberian Polar Current, river runoff and the effect of the Bay of Biscay on thermal stratification) on the spatial differences in the seasonal signal and the interannual variability is discussed.

Resumen

El estudio analiza una serie temporal de datos de temperatura de la superficie del mar (TSM o SST en inglés) procedentes del sensor AVHRR (Advanced Very High Resolution Radiometer, en inglés) de los satélites NOAA/NASA, Pathfinder V5, y datos del sensor MODIS (Moderate Resolution Imaging Spectroradiometer, en inglés) del satélite Aqua, sobre la Plataforma Septentrional Ibérica, cubriendo el periodo 1982-2012. El análisis ha sido realizado a través de una función empírica ortogonal (EOF en inglés) con el fin de poder definir un patrón espacio-temporal, la magnitud de variación estacional, así como la variación interanual de SST. En la Plataforma Septentrional Ibérica (NIS en inglés), la Componente Principal número 1 (Principal Component 1 o PC1, en inglés), representa más de un 90% de la variabilidad de datos., Los loadings muestran una señal cíclica estacional muy fuerte y unos scores espaciales con gradientes conspicuos a lo largo del área de estudio. El patrón temporal ha sido también observado a gran escala en el Sudeste Atlántico Europeo. (SEA en inglés). El análisis de los patrones espaciales indica que la SST en verano en la Plataforma Septentrional Ibérica es baja y se va incrementando a lo largo de la Plataforma Cantábrica, llegando a ser máxima en el interior de la Bahía de Vizcaya. Sin embargo, este proceso se invierte durante el invierno, en que la temperatura es máxima en la Plataforma Septentrional Ibérica y decrece hacia la Plataforma Cantábrica, llegando a ser mínima en el interior de la Bahía de Vizcaya. Ello indica que existe una fuerte variación espacio-temporal de la SST en el área de estudio. Además la comparación entre las dos plataformas NIS y SEA, permite realizar hipótesis sobre la naturaleza de los procesos que probablemente estén gobernando la variabilidad interanual en la NIS, i.e. variaciones similares en ambas áreas podrían corresponder a fuertes procesos de gran escala, mientras que la existencia de diferencias entre NIS y SEA podrían ser indicativas de que están ocurriendo procesos de mesoescala en la propia NIS. Dichos procesos son comentados en los diferentes espacios, signos estacionales así como variaciones interanuales.

1.   Introduction

The remote nature of remote sensing technology allow us to make observations, take measurements (i.e. measuring the reflected and/or emitted electro-magnetic energy from the earth's features), and produce images of phenomena that are beyond the limits of our own senses and capabilities. It was the launch of the first civilian remote sensing satellite in the late July 1972 that paved the way for the modern remote sensing applications in many fields including oceanography (Lillesand *et al.,* 2004).

Satellite remote sensing provides a large amount of data at different spatial, spectral, and temporal resolutions by using appropriate combination of bands to bring out the natural and man-made features that are most pertinent to a certain project for detecting changes. The data obtained from satellites imagery used for a wide array of change related application areas such as vegetation and ecosystem dynamics, hazard monitoring, hydrology, oceanography and so on. Satellite image data enable direct observation of the land and sea surface at repetitive intervals and therefore allow mapping of the extent, monitoring and assessment of changes exhibited by land and sea surface phenomenas (Lillesand *et al*., 2004).

The availability of such data has given researchers the possibility to investigate oceanographic regions in a manner that were previously very difficult or impossible. In the last four decades, the measuring of the oceans from space has greatly improved the knowledge of the oceans by providing a synoptic and continuous view for monitoring the oceanographic environment. The oceans are a dynamic environment therefore, continuous monitoring is necessary in order to capture the changes of the parameters of interest. Remote Sensing is an excellent method to monitor such dynamic environment. The obvious advantage of remote sensing is the gain of perspective and, possible use of historical data and a continuous monitoring by regular revisits of satellite sensors.

One of the key data products of satellite image is Sea Surface Temperature (SST). The spatial and temporal variability of SST reflects the dynamics of physical

processes operating at different temporal and spatial scales (Mann & Lazier, 1996). In mid-latitude temperate areas, SST presents a remarkable seasonal pattern forced by the seasonal variation in solar radiance and atmospheric temperature which also reflects the pattern of thermal stratification of the water column. In winter, SST is low and the sea surface layer (circa (c.) 100 m) presents homogeneous density that facilitates vertical mixing. As SST increases in spring there is a concurrent thermal stratification of the water column in the vertical dimension and the thermocline (the strongest gradient of temperature) progressively deepens. In autumn, the decrease in atmospheric temperature and the increase in wind speed associated to more frequent storms cause the decrease in SST. As SST decreases, vertical mixing is enhanced and thermal stratification reduced until well mixed conditions are reached in winter again. This process explains SST patterns at large latitudinal gradients depending on seasonal variation in atmospheric temperatures and storm associated to low pressure systems. The alternation between vertical mixing in winter and stratification in summer also regulates the seasonal dynamics of phytoplankton production and its transference towards different trophic pathways of the food web (Legendre & Rassoulzadegan, 1996). At shorter spatial scales (e.g. mesoscale c. 10-10000 km), however, other physical processes interact with this seasonal process and modulate SST patterns. In extreme cases these mesoscale processes can even dominate the forcing of SST. Coastal upwelling is possibly the most apparent case of mesoscale process, due to its consequences in the hydrodynamics and in ecosystem characteristics, with important associated fisheries. Equatorward winds parallel to Eastern continental boundaries provoke the offshore displacement of surface waters which are therefore replenished by the upwelling of subsurface cold, nutrient rich waters. This process is the consequence of wind forcing onto the surface layer and the Coriolis effect. The water mass displacement forced by the along-shore wind can be decomposed in a vector parallel to the coast line and another perpendicular, which therefore causes an offshore net transport of coastal water masses. The upwelling of deep nutrient-rich waters in areas of permanent stratification (subtropical areas) or during summer stratification increases primary

9

production and, moreover, its transference towards higher trophic levels. The major Eastern Boundary Current Systems, i.e. the California Current, the Humboldt Current, the Canary Current and the Benguela Current account for less than 1% of ocean surface and more than 25% of world annual fisheries catches (Pauly & Christensen, 1995). Other mesoscale processes that can affect SST and ecosystem production are river plumes, internal waves, and frontal structures in general.

With the increasing availability of satellite SST data, it has become possible an integrated monitoring of temporal and spatial variation in SST. This data improve greatly from the very limited spatial data offered by ship observations.

In interpreting the long-term time series datasets such as SST, it is very common practice to use different statistical methods. These methods can extract the intrinsic features and characteristic which may be varying with the time and spatial scale (Tarumay *et.al., 2004*). Generally, there are routine archives that have been used to analyze time-series variability of SST (Galladudet & Simpson, 1994). Among the methods available, the empirical orthogonal function (EOF) analysis has been a particularly useful tool in studying large quantities of multivariate data (Galladudet & Simpson 1994, Keiner & Yan 1997, Lagerloef & Bernstein 1988). This method decomposes a time-series data set into its orthogonal component modes, of which the first few can be used to describe the dominant patterns of variance in the time-series.

The emphasis of this study was the use of SST data acquired from Pathfinder Version 5 (V5) and MODIS Aqua sensors for the investigation of spatial and temporal variability in the marine environment. A time series analysis was performed upon the data using open source R statistical software in order to reveal the mean monthly SST variability in the study area. R is an excellent tool for manipulation, analysis and visualization of geographically data such as SST satellite imagery compiled in a Network Common Data Form (NetCDF) file format (R Development Core Team 2009).

In this thesis, remotely sensed data was used to describe the variability of SST in the Northern Iberian shelf.

2. Objectives

A time series analysis, EOF (Jensen, 2005; Eastman & Fulk, 1993) has been performed on SST data sets. The EOF analysis in these data will produce both spatial and temporal outputs suggesting where the SST varies over time in the study area and the relative magnitude of those variations. The outputs are called principal component images (explaining spatial variations) and principal component loadings (explaining temporal variations). The goal of such analysis is not to describe the average conditions in the area over time, but merely a mapping of the variations from the average SST variation over time.

The study was restricted to the shelf, as the slope establishes a clear boundary on the influence of mesoscale forcing. The higher influence of mesoscale forcing, which increases primary production and, moreover, modulates its seasonal pattern, is the ultimate cause of higher fisheries production associated to shelf seas compared to the open ocean. This study is intended as a preliminary analysis of the long-term physical variability of the North Iberian shelf ecosystem.

The objectives for this study are:

1. To analyze the spatial pattern, timing and relative magnitude of seasonal and interannual variability of SST in the Northern Iberian shelf using EOF analysis.
2. Interpret these patterns according to the dominant oceanographic processes in the area.
3. Identify years with higher than average or lower than average seasonal patterns as potential events for ecosystem variability.

3. Materials and Methods

3.1 Study area

The area of study comprises the Northern Iberian shelf north of 41°00'N, which includes the Northern most Portuguese shelf, the whole Cantabrian shelf, from Cape Estaca de Bares to the French border, and a small area of the southernmost French shelf of the Bay of Biscay south of 44.2° N, 1.5° W. The area is characterized by a relatively narrow shelf with a mean width between 30 and 40 km and as narrow as 12 km in the Eastern Cantabrian (Figure 1).

The continental shelf is characterized by a progressive decrease in depth down to approximately depth of 150 m where the continental slope begins, consisting in a very sharp decrease in depth down to 1000 m. Further offshore depth continues to decrease but a lower rate until the deep basins of the oceanic platform reach maximum depths of c. 4500 m. In this study the shelf was delimited by the area inshore of the 500-m isobath.

Nogueira & González-Quirós (2011) describe the general climatic and oceanographic characteristics of the area as follows: "The climate at North Ibearian coast is classified as oceanic (Cfb in the Köppen climate classification system), characterised by relatively cool summer and warm winters, with a narrow annual temperature range (c. 10 °C) and precipitations evenly dispersed around the year. Southward from Cape Finisterre, the climate is still oceanic but with increasing Mediterranean character (Csb), characterized by warm to hot, dry summers and mild to cool, wet winters. The mean of the total annual precipitation varies from 1800 mm year^{-1} in the Northwestern Galician coast to less than 1000 mm year $^{-1}$ in the Eastern Cantabrian. The wind pattern is governed by the position of the two main centers of activity in the North Atlantic: the anticyclone south of 40°N (the Azores High) and the low pressure area centered around 60°N (Iceland Low). Between these two areas, the prevailing winds are relatively strong from the west and southwest in winter. In summer, the northward displacement and reinforcement of the Azores High give rise to a predominance of equatorward

coastal winds that promote coastal upwelling in Galicia, with decreasing intensity eastward along the Cantabrian coast. Besides, the development of thermal lows in the Iberian Peninsula reinforce northerly winds, which can sometimes reach near gale force during the afternoon as a result of the intense heating over the continent (OSPAR 2010)".

Most of the water masses in the study area are of North Atlantic origin, including those that have been transformed after mixing with the Mediterranean water. Depending on latitude, the region is affected by both the subpolar and the subtropical gyres, but the general circulation in the area mainly follows the subtropical anticyclonic gyre in a relatively weak manner. The circulation off the western coast of the Iberian Peninsula is characterized by a complex current system subject to strong seasonality and mesoscale variability, showing reversing patterns between summer and winter in the upper layers of the shelf and slope (e.g. Barton, 1998; Peliz et al., 2005). During spring and summer northerly winds along the coast are dominant, causing coastal upwelling and producing a southward current at the surface and a northward undercurrent at the slope (Fiúza et al., 1982; Haynes & Barton, 1990; Peliz et al., 2005; Mason et al., 2006). In the Cantabrian Sea the surface currents generally flow eastwards in winter and early spring and change westwards in late spring and summer following the windforcing (Lavín et al., 2006).
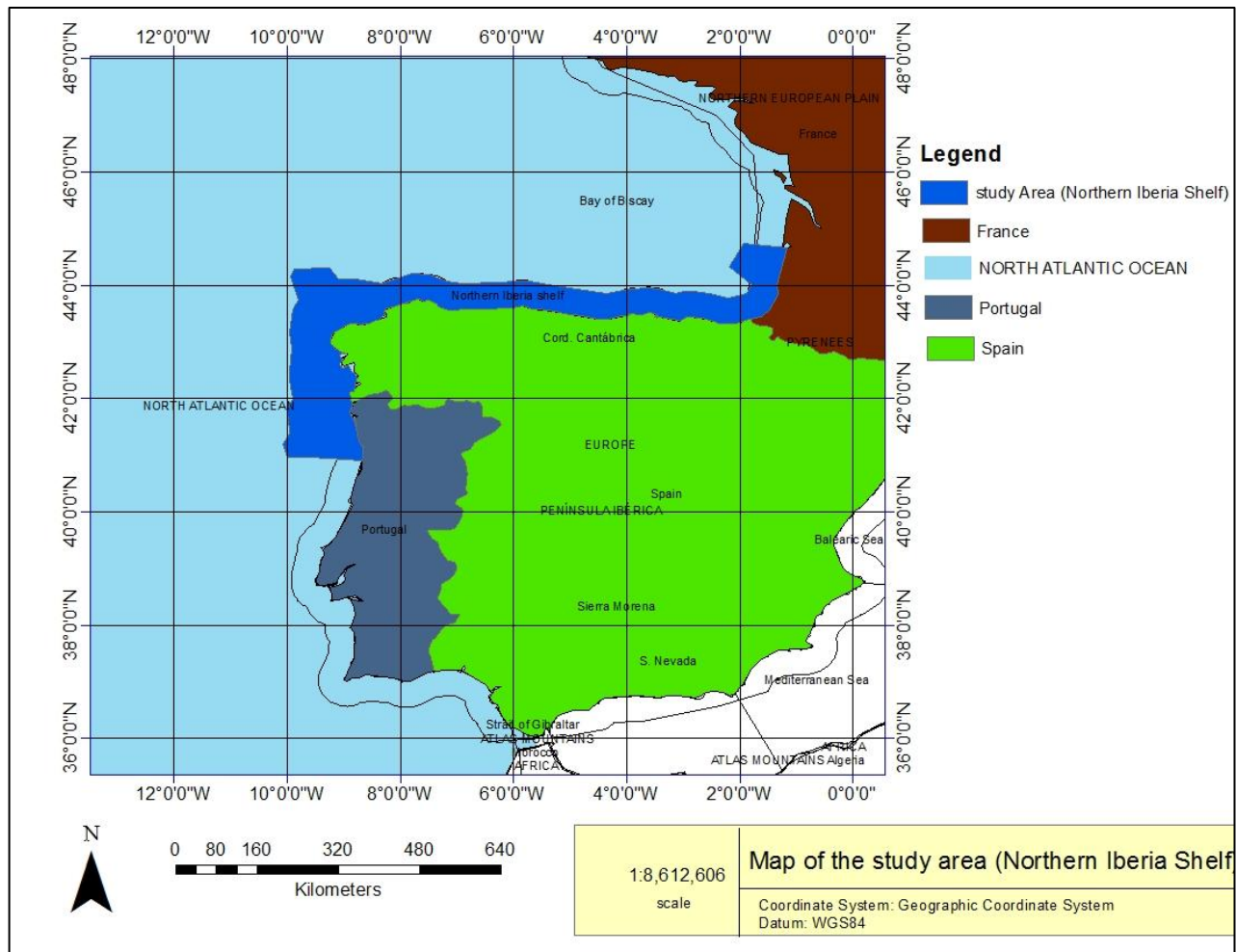
Figure 1. Map of Study area Northern Iberian Biscay Shelf

3.2 Satellite data

SST data between the geographical location of 36°N to 48°' N latitude and from 15° to 0° West longitude were obtained from level 3 satellite images of two different sensors:

1. Pathfinder Version 5.0 monthly composite of SST with a spatial resolution of 4 km and a temporal coverage from January 1st, 1982 to December 31st, 2009 were downloaded from the Environmental Research Division's Data Access Program (ERDDAP:http://coastwatch.pfeg.noaa.gov/erddap/griddap/erdPHsstdmday.html), which is part of the National Oceanic and Atmospheric Administration (NOAA).

The Pathfinder Version 5.0 SST data set is a reprocessing of global SST data from NOAA's Advanced Very High Resolution Radiometer (AVHRR) aboard NOAA's Polar Operational Environmental Satellite (POES). This reprocessing task provides a long-term continuous data series for use in climate research as well as other application requiring the highest quality of data.

According to ERDDAP, in the POES Global Area Coverage SST dataset, AVHRR radiance measurements are subsampled aboard the satellite and downloaded to receiving stations at 4-km resolution. Pathfinder processing uses a modified version of the non-linear sea surface temperature (NLSST) algorithm (Walton et al., 1998), with changes outlined in Kilpatrick et al. (2001). Changes in the algorithm include: an improved atmospheric correction, superior cloud masking, and monthly recalculation of algorithm coefficients based on a match-up database of in situ SST measurements (moored and drifting buoys). SST data is available from 1982 to 2009 at 4-km resolution and SST values are accurate to within 0.3 degrees Celsius. The data are mapped to an equal angle grid (0.05 degrees latitude by 0.05 degrees longitude) using a simple arithmetic mean to produce individual and composite images of various durations (e.g. 8-day and monthly).

2. MODIS Aqua monthly composite of SST with 4 km resolution and temporal coverage from January 1st, 2003 to December 31 st, 2012 were downloaded from the Environmental Research Division's Data Access Program (ERDDAP: http://coastwatch.pfeg.noaa.gov/erddap/griddap/erdPHsstdmday.html).

CoastWatch offers sea surface temperature measurements from the Moderate Resolution Imaging Spectroradiometer (MODIS) sensor on NASA's Aqua spacecraft. The Science Quality SST concentration product is an improved version of the near real time SST products.

Data are made available at approximately 5.5 km resolution for the global oceans. MODIS SST is accurate to within ±1 degree Celsius, and SST values are validated by comparison with buoys temperature data from the National Data Buoy Center. The data are mapped to an equal angle grid (0.05 degrees latitude by 0.05 degrees longitude) using a simple arithmetic mean to produce composite images of various images (1, 8-day and monthly).

The reason why two different data sets with different temporal and spatial resolution are used is that we could not find a continuous science quality SST data set of the desired temporal coverage from a single sensor.

Both products were available in NetCDF format. The downloaded SST data were read and further processed using R-software.

3.3 Data preprocessing

To perform an Empirical Orthogonal Function Analysis it is necessary to have a complete data set for each pixel, but the downloaded satellite data had small gaps with no data in regions with persistent cloud clover. It is clear that the data gaps must be filled such that each image contains continuous data. The data used for filling the holes in the images have to be representative. The methods used must be as close to reality as possible in order to be usable. The approach to tackle this problem was backfilling.

Backfilling of data into the areas of missing values can contribute greatly to a data set's completeness. Spatially filtered data can be backfilled onto the original image where only the newly calculated values from the filtering process is put back onto the original image. This method can be said to have high significance for the areas of missing values because the filtered backfill data was calculated directly from the image that was backfilled. This process was implemented separately for both datasets, Pathfinder V5 from 1982 to 2009 and MODIS from 2003 to 2012, as follows.

First, for each month of the year, all data corresponding to that month in the time series were averaged, resulting in an initial climatology consisting of 12 monthly means (Annex 1). Then the gaps in the original image were filled with the mean value of the surrounding SST values by a filter box of 3 X 3 pixel centered on the missing value pixel (nearest neighbor). Only few pixels were missing after the fifth iteration, and each of these pixels was backfilled with the corresponding pixel monthly climatology. The result was a complete time series of monthly data with no missing data due to cloud cover (Figure 3).

After filling the missing pixel values of both types of images, the Pathfinder image from January 1st, 1982 to December 31st, 2009 and only the three years of MODIS image from January 1st, 2010 to December 31st, 2012 were merged in order to have one continuous time series matrix. For the convenience of computation and analysis, the Pathfinder SST data were resampled to have the same spatial resolution as the MODIS SST data. Then the study area Northern Iberia Shelf was delimited by the area inshore of the 500-m isobath. There were a total 103033 spatial data points and 372 monthly (31 years) temporal images over the study area. Figure 2 illustrate the flowchart of the methodology employed in this   study.
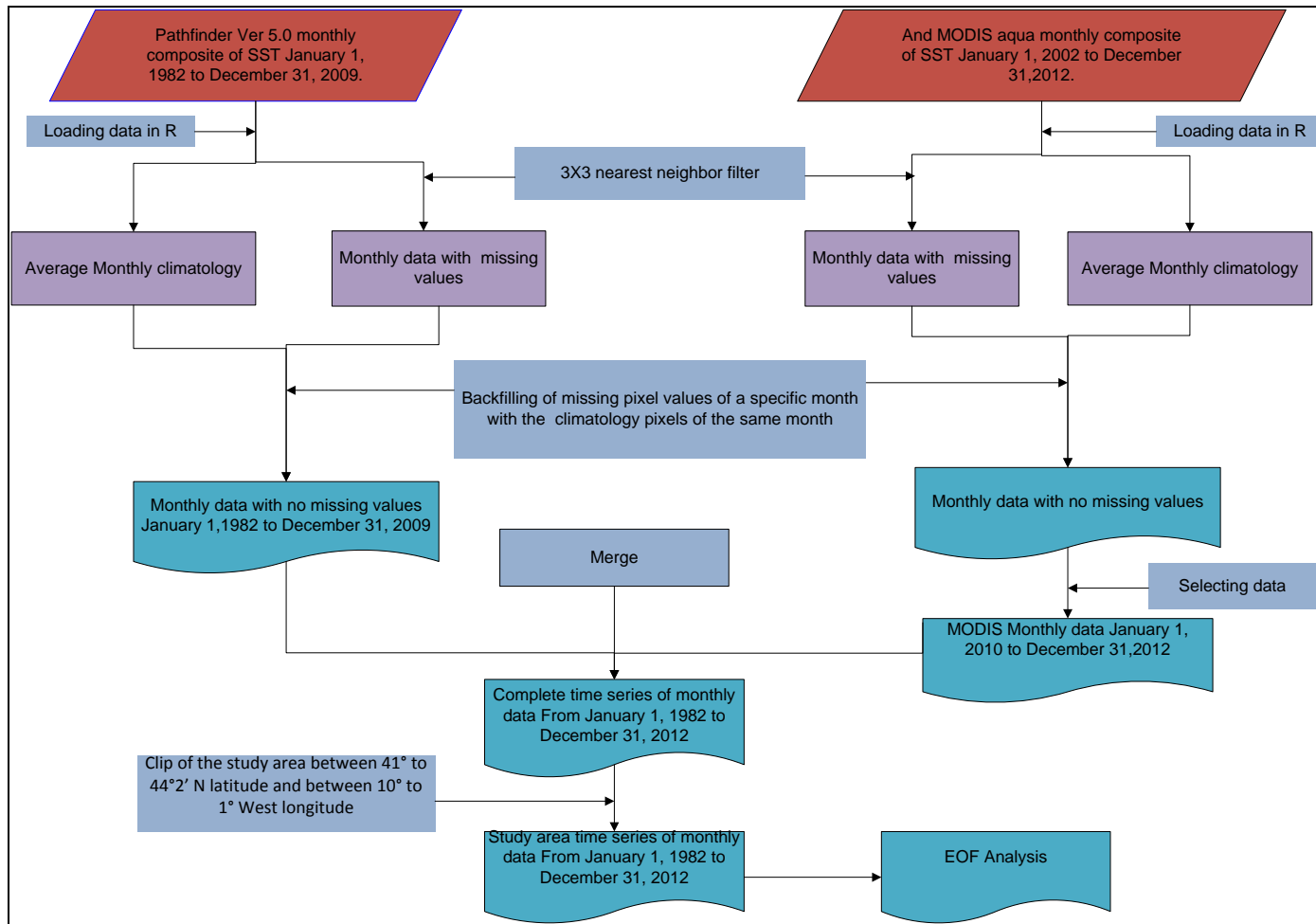
Figure 2. Flowchart showing the process flow from Level 3 raw data to the Time Series Analysis.
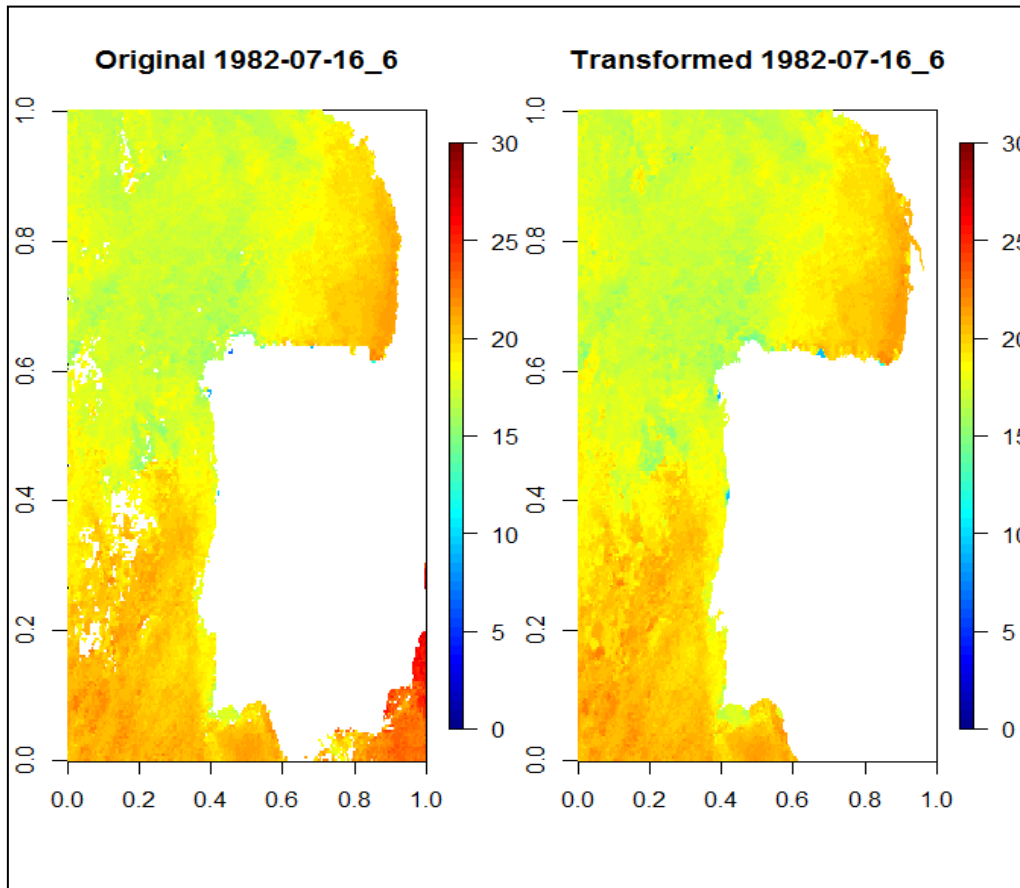
Figure 3. Original to the left and backfilled to the right of monthly SST of July 1982. (X – axis and Y-axis Indexed Grid and SST in °c)
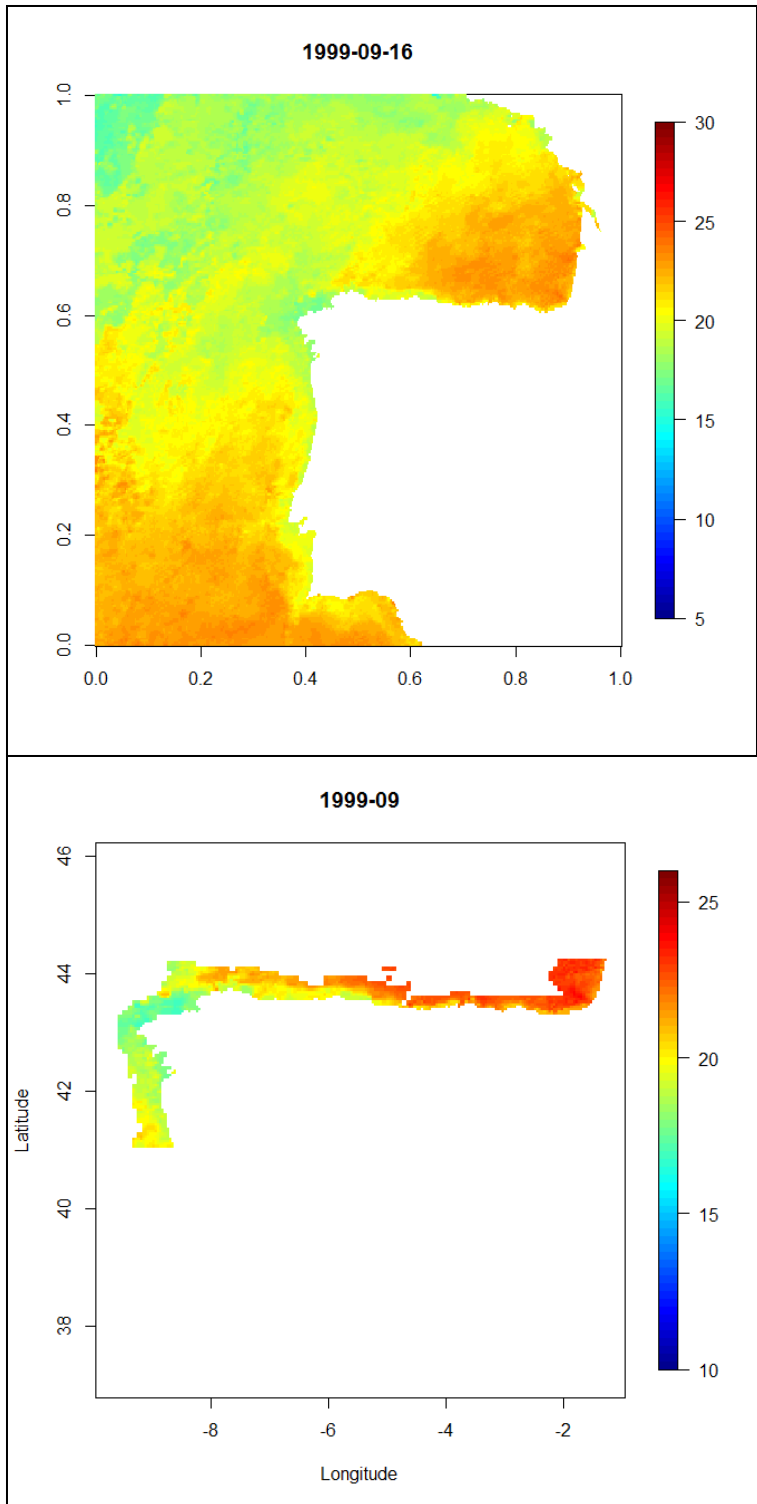
Figure 4. The study area delimited from the general data set (above) by the area inshore of the 500-m sobaths (below). (Latitude (°), Longitude (°)and SST in °c)

3.4 Time Series Analysis

A time series analysis was performed upon the data within R environment in order to reveal spatiotemporal SST variation in the study area. R software was considered the most suitable for analyzing the vast amounts of remotely sensed data needed in this study. This is because R offered suitable time series analysis of remotely sensed data. Moreover, the downloaded data was in netCDF files format, which was easier to analyze in R software than Geographical Information System (GIS) software.

The analysis was performed in two different domains: (1) the Northern Iberian Shelf (as delimited in Figure 4 the area between 41° to 44°2' N latitude and between 10° to 1° West longitude) and (2) the Southeastern Atlantic Ocean, between 36° to 48° N latitude and east of 15° W and west of the Strait of Gibraltar.

Dominant time space patterns of Sea Surface Temperature variability over the study area during the period of interest are quantitatively summarized using a standardized principle component analysis (SPCA). In Oceanography, this time series analysis technique is known as Empirical Orthogonal Function (EOF) (Emry & Thomson, 1997). In this study, the term EOF was used.

The general objectives of an EOF are: (1) data reduction while retaining as much variability as possible and (2) interpretation of large data sets. When dealing with large data sets with numerous data layers, it is almost impossible to keep track of the variations from layer to layer just by visible interpretation. In our case, dealing with 31 years of monthly SST data, it is difficult to describe the spatiotemporal variability of SST visually. A purely visual descriptive approach of each image is not sufficient or practical to reveal information from the data sets. It can be valuable to describe the spatial variations at specific times, but this is not the focus in this thesis. Focusing on specific snapshots of an area does not tell anything of how a system is varying as a whole; it only gives information of what the situation is at a particular time. From this point of view, it must be argued that

an EOF is a more appropriate approach for revealing patterns over time and space. This is because this statistical technique can analyze both space and time components, which make the EOF useful.

EOF analysis is a statistical method used to decompose a multi-variate data set into its principal components. Using this method, the bulk of the variance of a data set can be described by a few orthogonal modes, so that the major properties of the data set can be more easily understood. As applied in this research, the original multi-variate data set was a time series of SST imageries that had two spatial dimensions (Latitude and Longitude) and one temporal dimension. In order to obtain the two dimensional matrix for the analysis, the columns of each image were stacked so that the image became a column vector. When these column vector images were placed together as sequential column, an M × N matrix was formed, where M is the number of elements in the spatial dimension, in this case the number of pixels in an image (103033 pixels), and N is the number of elements in the temporal dimension, in the case the number of images (372 mean monthly images). Generally, the time-series of images can be represented by a linear combination of the eigenfunction (Fn) (Equation 1):

$$T(x,t) = \sum_{n=1}^{N} a_n(t)F_n(x) \qquad (1)$$

Where x and t were the spatial and temporal indices, respectively and a_n is the temporal amplitude or eigenvector. The eigenfunctions (F_n), or spatial amplitude functions, can themselves be viewed as images, giving a visual representation of the variance of each mode.

In order to extract more detail information from EOF analysis, Paden et al., (1991) suggested to standardize the variables prior to EOF analysis. The removal of the temporal and spatial means (standardizing the variables) revealed features that vary strongly in time and space, respectively. The temporal mean was removed by finding the mean over the time-series at each pixel (i.e. in each row of T(x, t)), and then subtracting the mean from each pixel in that row (Equation 2):

$$T'_t(x,t) = T(x,t) - \frac{1}{N}\sum_{i=1}^{N} T(x,t) \qquad (2)$$

The spatial mean was removed from T(x, t) by calculating the mean of each image (column of T(x, t)), and subtracting it from each pixel in that image (Equation 3):

.

$$T'_s(x,t) = T(x,t) - \frac{1}{M}\sum_{i=1}^{M} T(x,t) \qquad (3)$$

The amplitude scores were estimated by Equation (4):

$$Z_t(x) = Z'(x,t) \times \sum_{t=1}^{n} a_n(t) \qquad (4)$$

where $Z_t(x)$ is the amplitude score of pixel x; a_n is the eigenvector; $Z'(x, t)$ is the standardized value of the data matrix $T(x, t)$ and N is the number of images.

Finally, both the temporal and spatial amplitude scores of T'(x, t) SST images were used to decompose the data matrix by using the EOF method for explaining the spatial and temporal patterns of sea surface temperature.

4. Result

4.1 Northern Iberia Shelf

The EOF analysis of the data was applied using the prcomp function of R on the Northern Iberia Shelf in the southwest of Atlantic Ocean between 41° to 44°2' N latitude and between 10° to 1° West longitude. The data ranges from January 1, 1982 to December 31, 2012. The result of EOF is a list containing the coefficients defining each component (sometimes referred to as loadings), the principal component (PC) scores (the rotated data) and standard deviation of each column of the rotated data (sdev). In this study, EOF found 372 principal components (new variables) which can explain the same information as the original 372 variables (the 372 mean monthly SST images). The next thing we wanted to know was how much each of the new variables has a power to explain the information that the original data have. For this, we need to look at Standard deviation and Proportion of Variance in the result Table 1.

	PC1	PC2	PC3	PC4	PC5	PC6
Standard deviation	139.8454	17.34621	14.18564	12.68998	7.29700	6.01672
Proportion of Variance	0.9372	0.01442	0.00964	0.00772	0.00255	0.00173
Cumulative Proportion	0.9372	0.95163	0.96127	0.96899	0.97154	0.97328

Table 1. The first six principal components of Northern Iberia Shelf monthly SST data set

EOF calculates the combination of the variables such that new variables have a large standard deviation. Thus, generally a larger standard deviation means a better variable. Another way to determine how many new variables we want to take is to look at proportion of variance. This means how much of the information that the original data have can be described by the new variables. For instance, with only PC1, we can describe 93.72% of the information the original data have.

If we combine and use PC1 and PC 2, we can describe 95.16% of them. Generally, 80% is considered as the number of the percentage that describes the data well. So, in this research, only PC1 was considered.

A plot of the first 10 principal component's variance is shown in Figure 5. The first principal component is dominant, and a very steep drop in variance follows for the rest of principal components. This indicated that there was a strong common time-varying signal in the data, which virtually overwhelmed any other temporal variability.
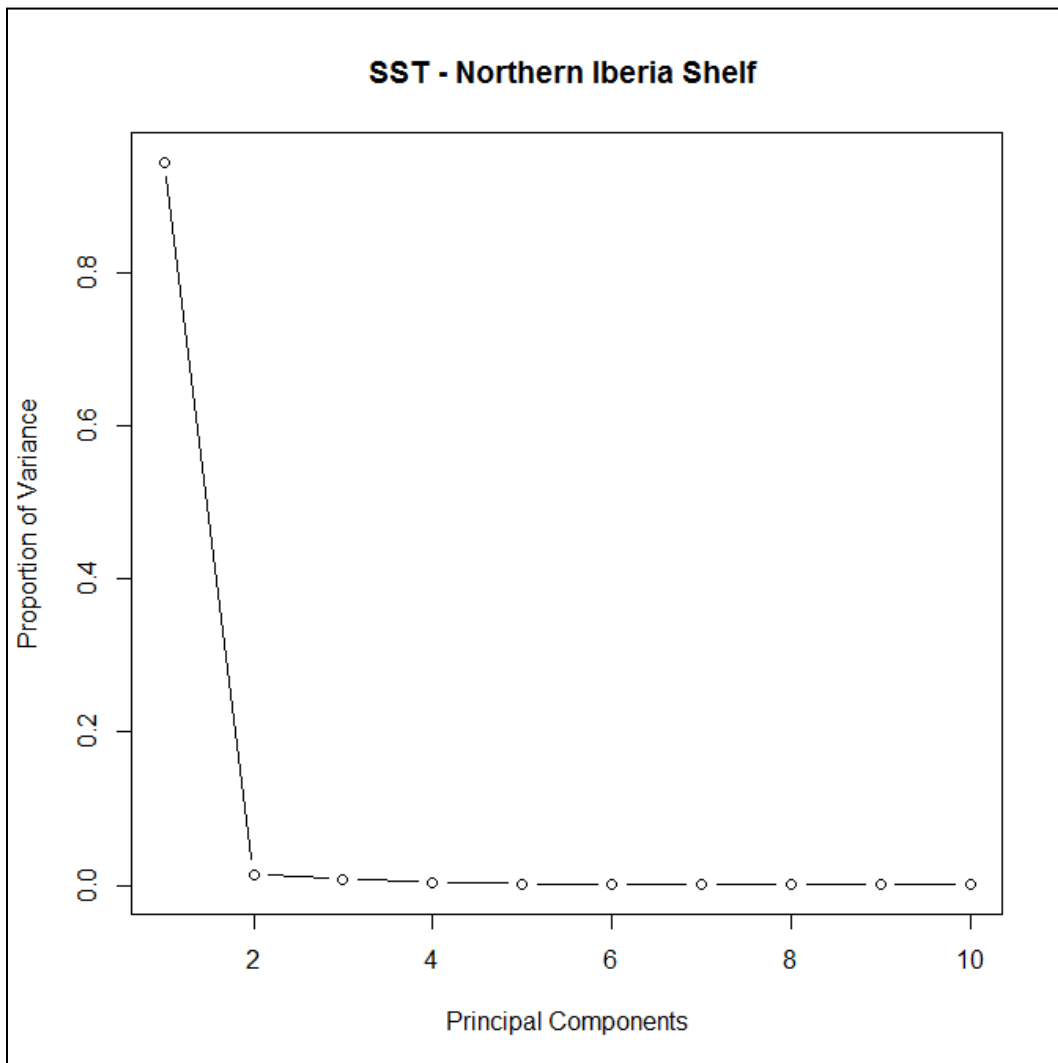

Figure 5. Plot of the variances explained by the principal components of the Northern Iberia data set.

4.1.1 Spatial variability

The first PC represent the characteristic of SST integrated over all the months in the times series. The amount of variation was 93.72 %. The scores illustrate the degree of correlation between each of the monthly images and the component that has been mapped. If a month shows strong positive correlation with a component image, this indicates that the month contains a spatial pattern that has strong similarities to the component image. A strong negative correlation indicates that the monthly image has a pattern that is the inverse of the component image. As noted by Eastman & Fulk (1993) the strength of a component is determined by both the magnitude of the variability it explains and the area over which that variability occurs.

The PC1 image gives information on where the changes indicated by the component loadings take place (Figure 6). All the pixels present positive scores in PC1, although the value progresively increases from the southern limit of the
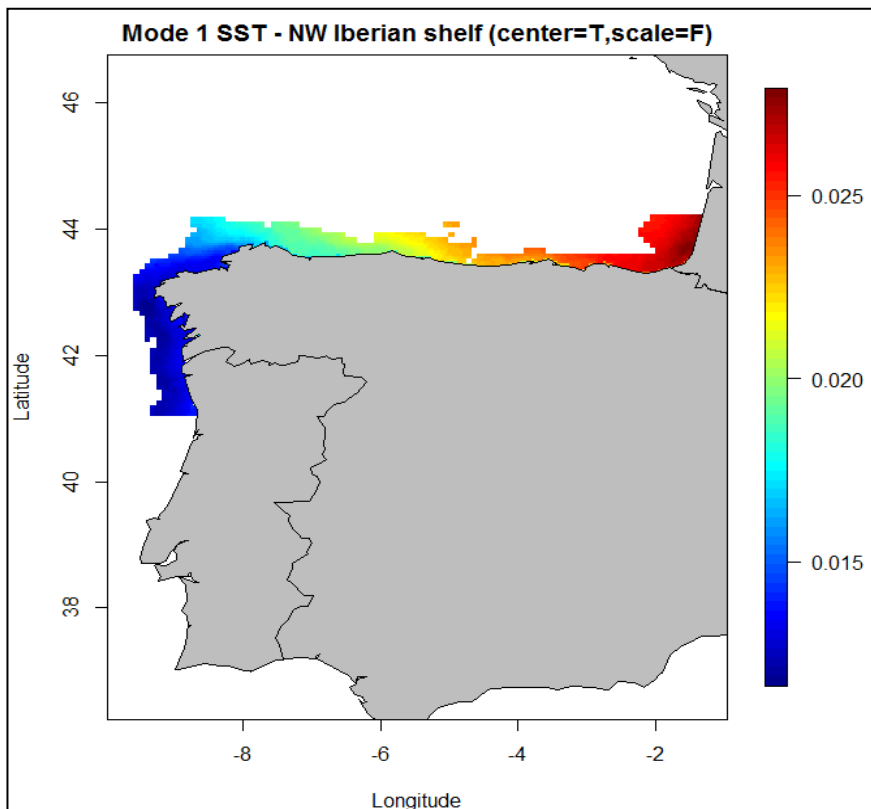

Figure 6. Score of PC 1 derived from monthly SST data of N Iberian shelf , January 1982 to December 2012 (Latitude (°), Longitude (°)and Z- axis score values)

27

Northern Iberian Shelf off the Portuguese coast towards the opposite limit of the domain at the inner Bay of Biscay.
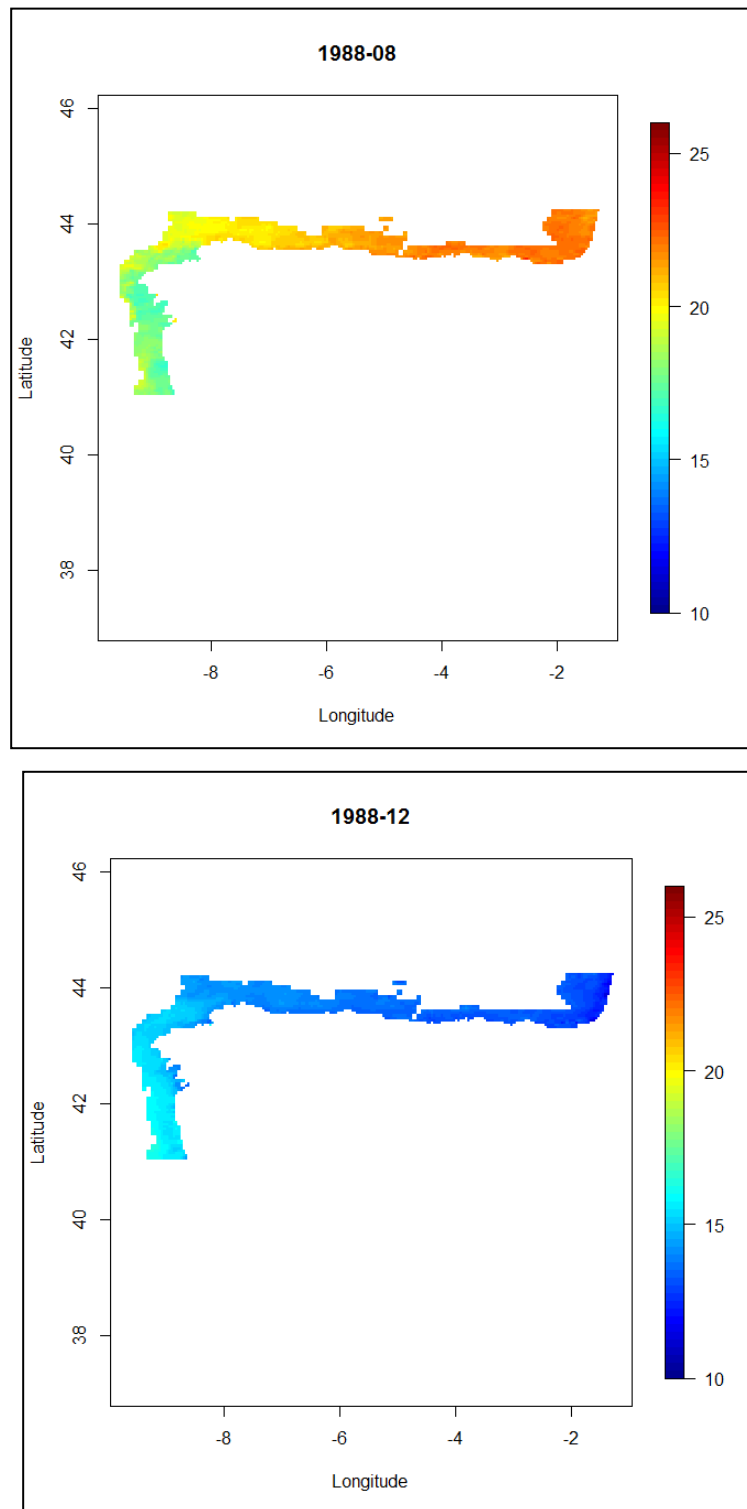

Figure 7. SST of Northern Iberia Shelf, August 1988 above and December 1988 below. (Latitude (°), Longitude (°)and SST in °c)

This spatial pattern of the scores represents the SST gradient observed during summer (briefly discussed in chapter 5). The mean SST in August at the western Iberian Shelf (Portugal and Galicia) is < 18ºC, it increases towards the North and thereafter towards the East along the Cantabrian shelf, with maximum temperatures > 20 ºC at the inner Bay of Biscay. Nevertheless and although less conspicuous, the spatial pattern of the scores also reflects the mean temperature distribution in winter. In winter, however, the thermal gradient in the area is of opposed signal to the pattern described during the summer. The mean SST in December at the western Iberian Shelf is > 13 ºC, it decrease towards the North and then towards the East along the Cantabrian shelf, with minimum temperatures < 13 ºC at the inner Bay of Biscay

4.1.2 Temporal variation

PC1 loadings show a strong seasonal signal (Figure 8), in which during winter the loadings have high negative values and during summer they have high positive value. However, this signal or pattern doesn't have equal magnitude from year to year. Figure 8 illustrated that, there are some years which had higher value of positive loadings and some had high value of negative loadings. This is a clear temporal pattern. The loadings graph begins in January 1, 1982, where the loadings are negative. In general, for each year, January, February, March, April, May and December has negative loadings and June, July, August, September, October and November has positive loadings.
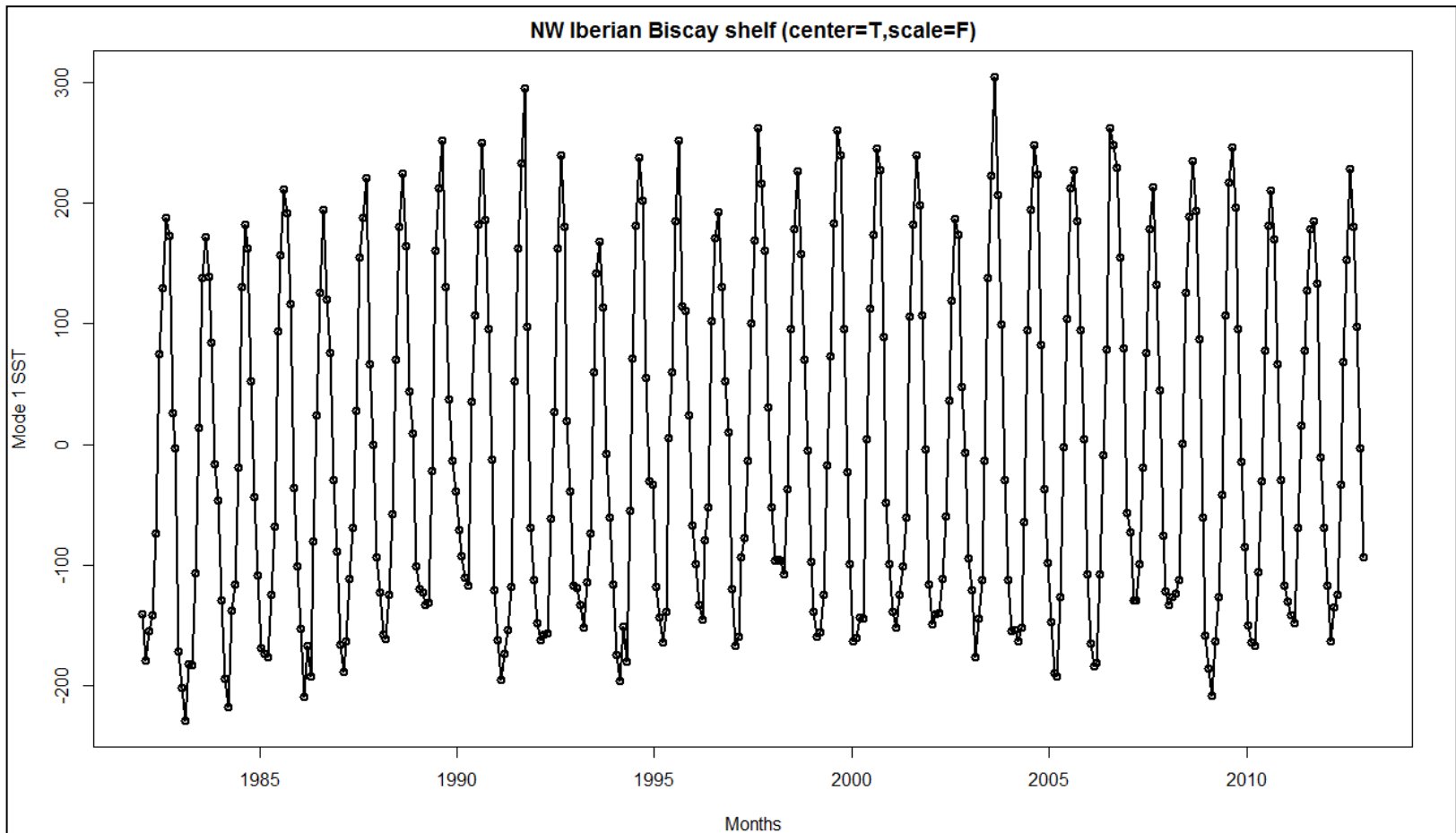
Figure 88. Loadings of PC1.

This phenomena show that there are seasonal variations throughout the time series. Moreover, the peaks of positive loadings are not the same for each month, nor are the magnitude the same for each peak. In 1987, 1991 and 2011 the peaks are in September and in 2006 the peak is in July, however, for the rest of the year the peaks were in August. The highest peak was in August 2003 followed by September 1992. There was also some interesting pattern in 2006, in which the three consecutive months July, August and September were high above the average peaks. The three lowest positive peaks were in August 1993, followed by August 1983 and August 2002.

There is also a variation in loadings and magnitude of the bottom peaks. The bottom peaks of March 2000, January 2003 and November and December of 2006 contain smaller negative loadings than the other months of bottom peaks through the time series. The timing of the peaks are calculated also differs slightly from year to year. The first component loadings show the interannual variation. Even if each year is similar to the other years there are some seasonal differences as indicated by the graph.

Another way of looking the data set is plotting the PC 1 loadings for each year (Figure 9 and 10). Figure 9 illustrated seasonal variation of SST in Northern Iberia Shelf during summer. We can see from the figure that August 2003 has the highest positive loading followed by September 1991 and July 2006. However, 2003 and 1999 have a sharp decline of SST after August and september respectively, whereas 2006 has more or less constant high loading from July to october. We can conclude that 2006 has the overall highest positive loadings from the series.

Figure 10 illustrated, in color, the highest negative values of loadings for Northern Iberia Shelf. The highest negative loadings observed during the winter of 1982 (December, January and February) and followed by the winter of 2008 and 1993.
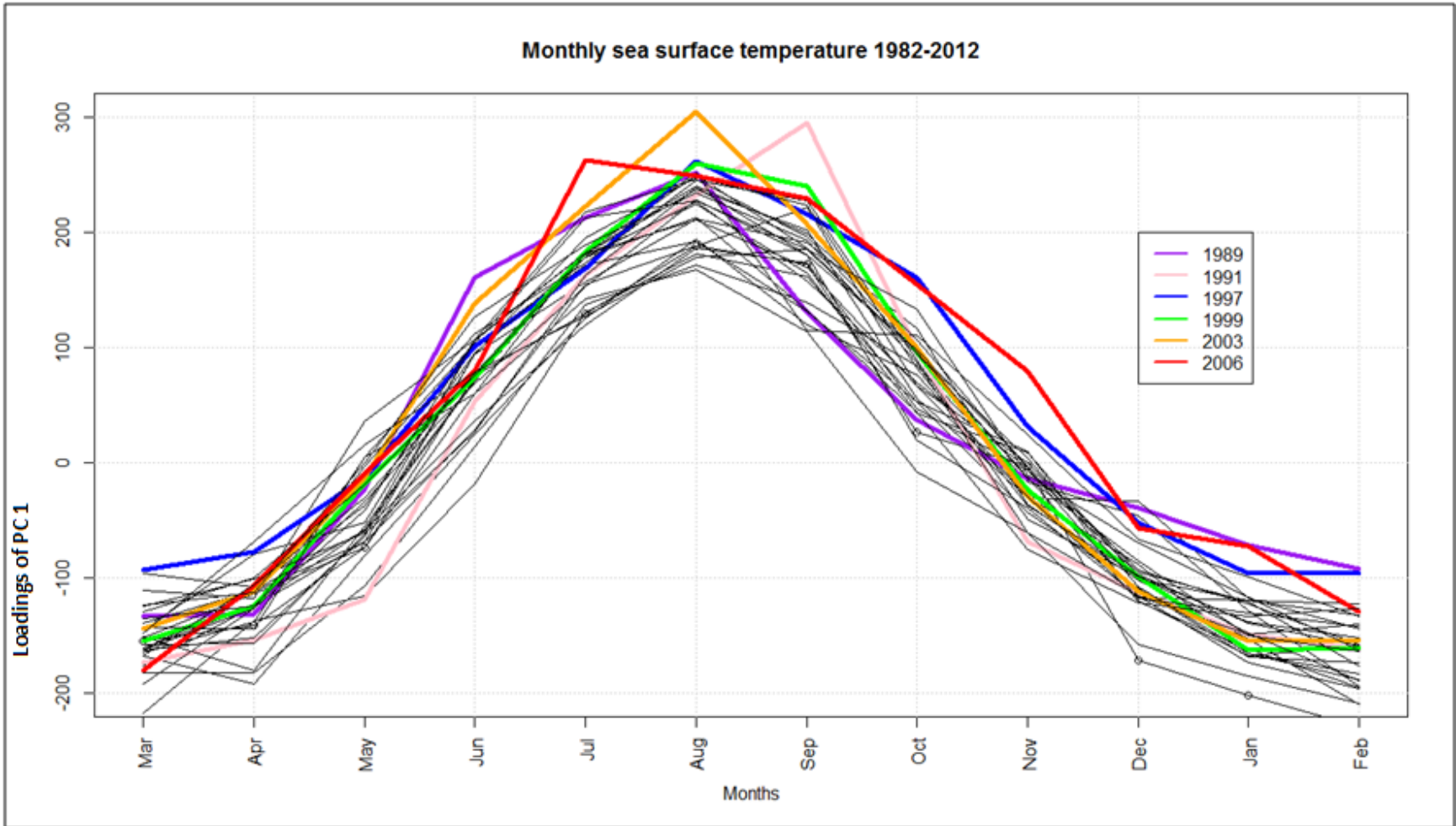
Figure 9. 9 Loading of PC 1 from year 1982 to 2012 showing high positive loadings in colors.
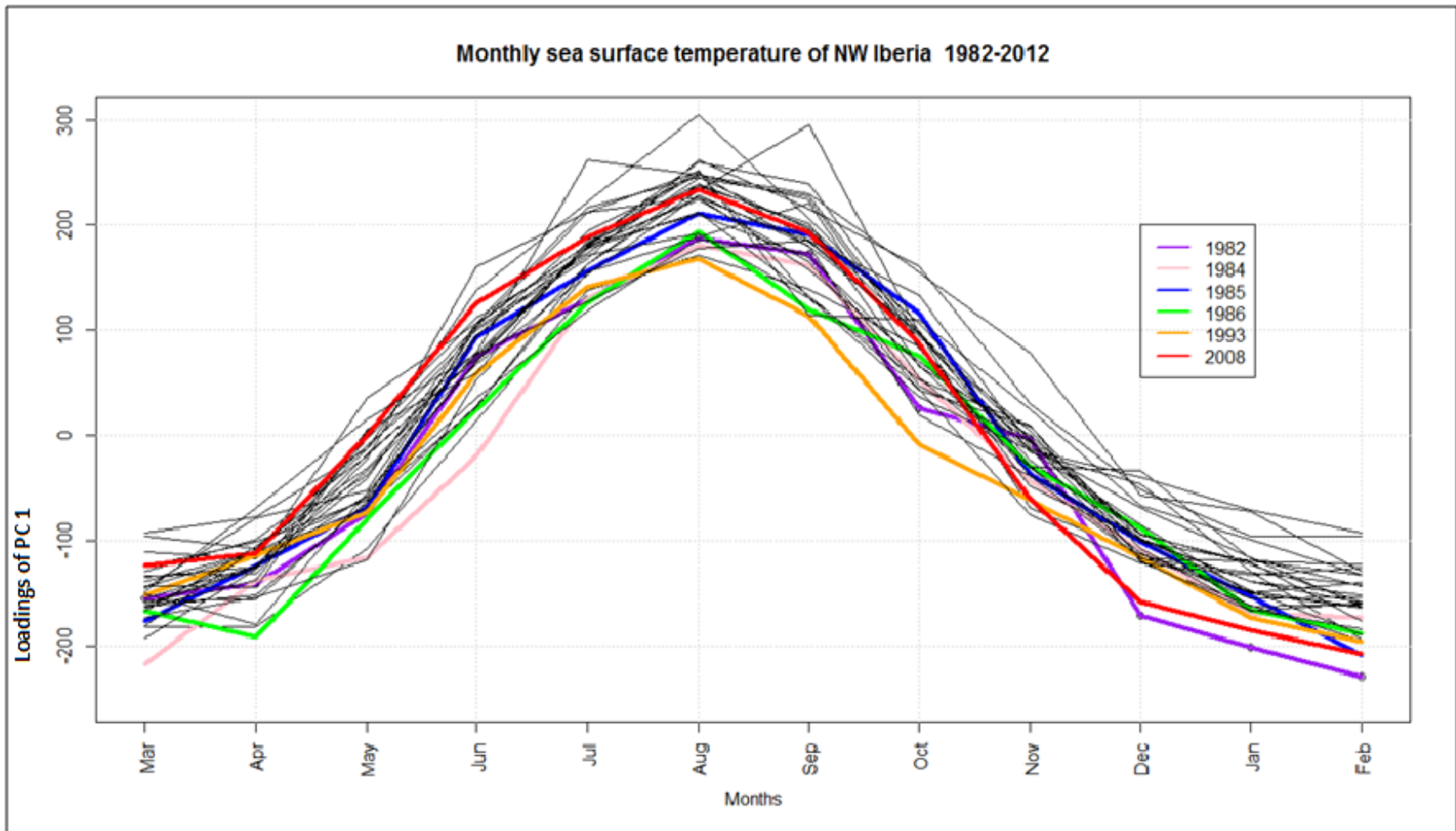
Figure 10. Loading of PC 1 from year 1982 to 2012 showing high negative loadings in colors.

4.2 Southeastern European Atlantic

The EOF analysis of the Southeastern European Atlantic (SEA) between 35° to 48° N latitude and between 15° to 1° West longitude carried out in the same manner as Northern Iberia Shelf. The dates range from January 1, 1982 to December 31, 2012. The result of EOF has 372 principal components. The first mode, representing about 94.38% of the variance, is largely predominant (Table 2) over the other PC's.

	PC1	PC2	PC3	PC4	PC5	PC6
Standard deviation	643.8071	78.93580	59.44224	39.64520	30.29178	25.20084
Proportion of Variance	0.9438	0.01419	0.00805	0.00358	0.00209	0.00145
Cumulative Proportion	0.9438	0.95800	0.96604	0.96962	0.97171	0.97316

Table 2. The first six principal components of the North East Atlantic Ocean monthly SST data set

A plot of the first 10 principal component's variance (Figure 11) also shows how the first component dominates this implies that the first principal component (PC1) is in good agreement with the original data. Because of these two reasons the first principal component is retained for the analysis.

.
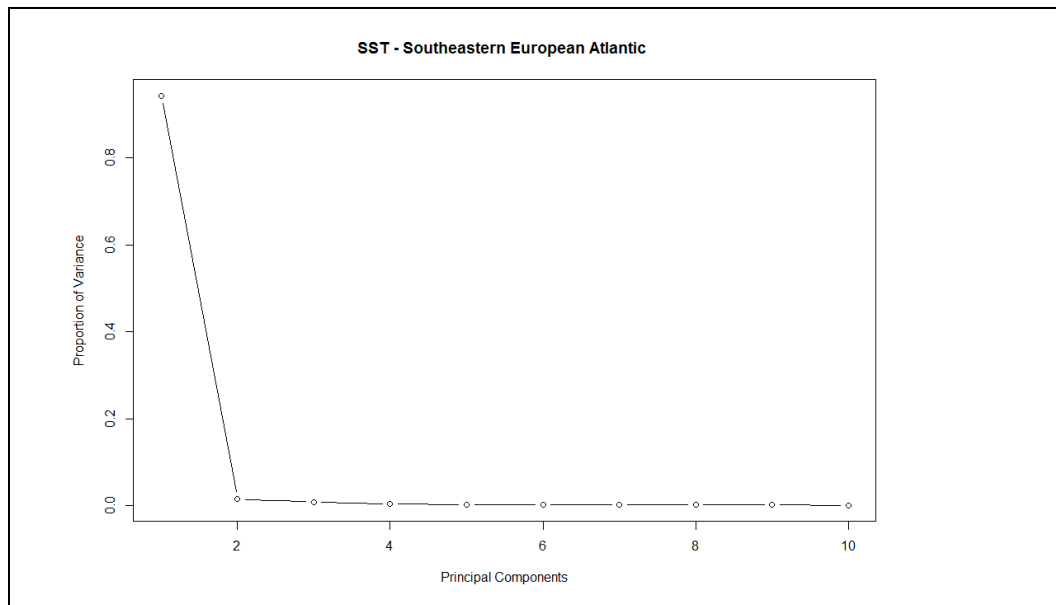
Figure 11. Plot of the variances explained by the principal components of the SEA data set.

4.2.1 Spatial variability

The PC1 image gives information on the spatial variability of SST exhibited in SEA (Figure 12). The areas with high positive correlation with the PC loadings are colored with red and the areas with high negative correlation with the PC loadings are colored in blue. According to the colors seen in the PC1 image (Figure 12), the Bay of Biscay has high positive correlation and coastal area of Portugal has high negative correlation, with the component loadings graph. The open ocean correlates less or has no correlation at all according to the image.

This explain that the coastal waters correlate stronger with the component loadings than the open waters since the relative change values are of higher values in the coastal zone than in the open waters.
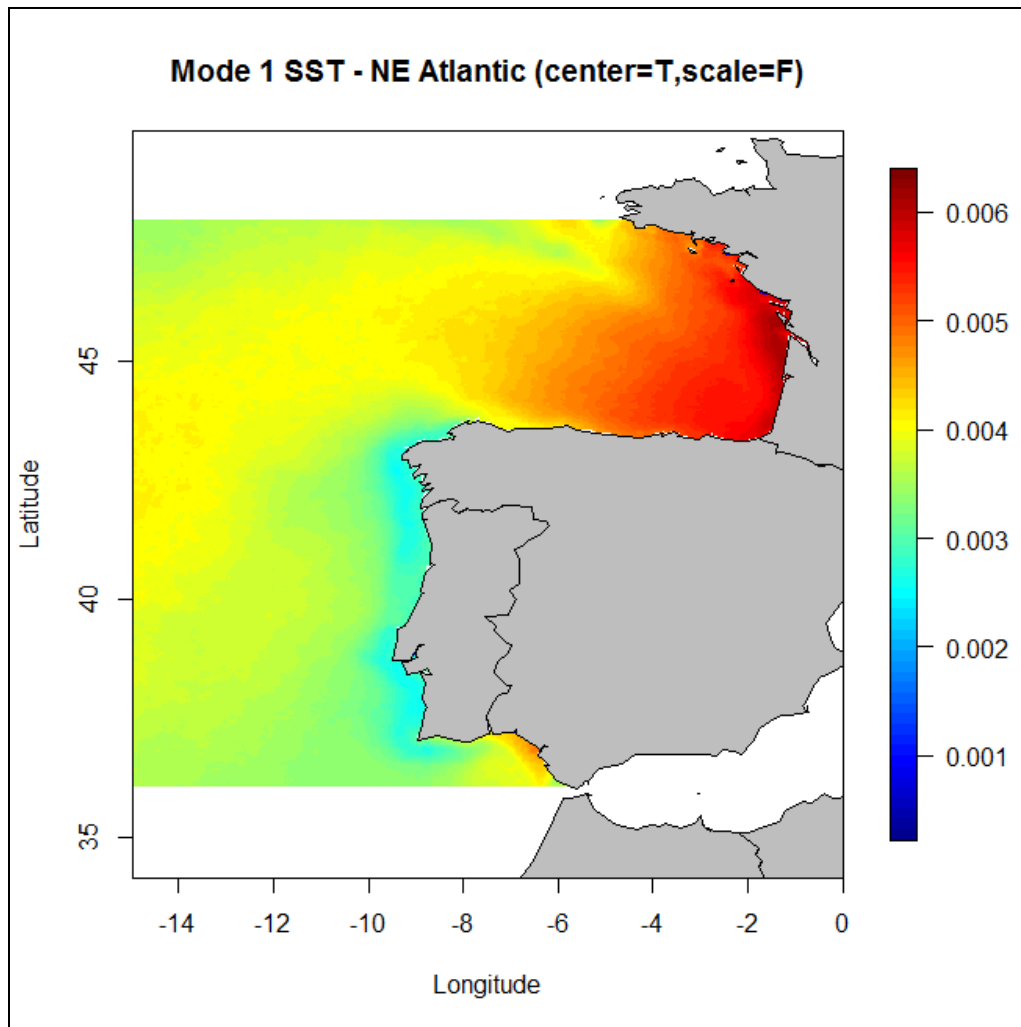
Figure 12. Score of PC 1 derived from monthly SST data of SEA, January 1982 to December 2012. (Latitude (°), Longitude (°)and Z- axis score values)
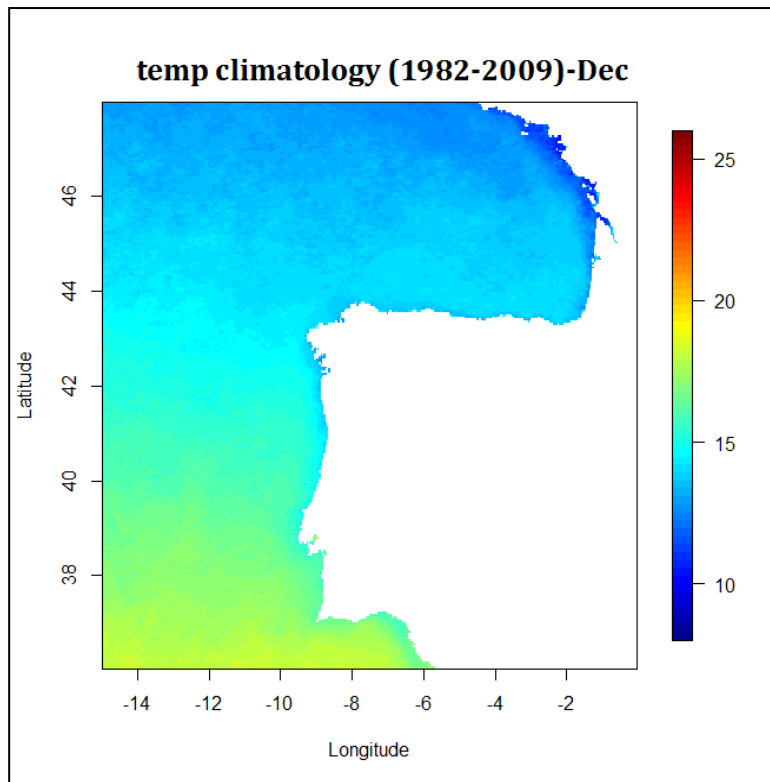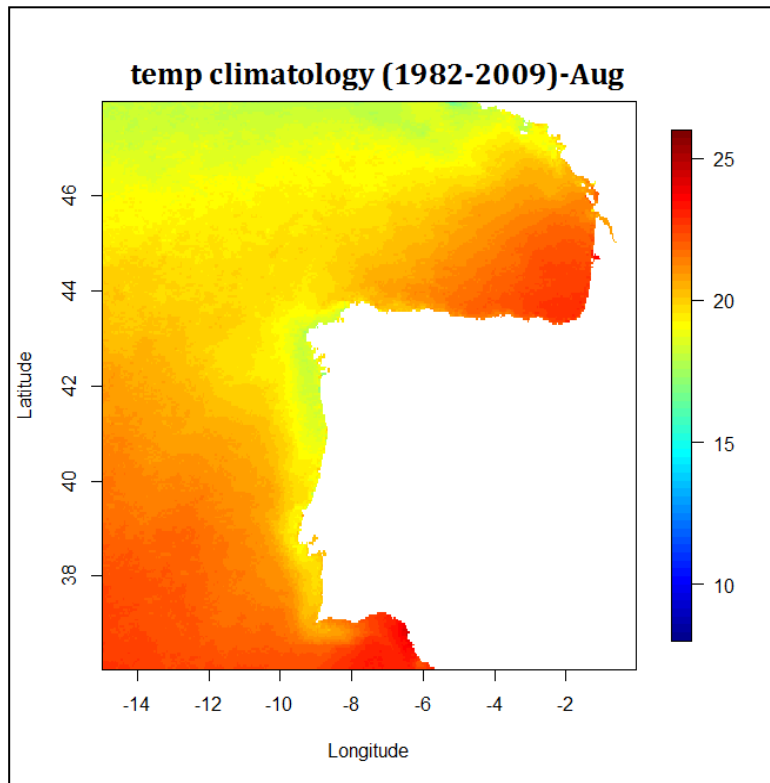
Figure 13. Mean SST of SEA August 1982 -2009 (above) and December 1982 -2009 (below). (Latitude (°), Longitude (°)and SST in °c)

We can see in Figure 13 that the Bay of Biscay has similar characteristics of SST variability with the southwest part of the open ocean during summer and with the north part of the open ocean during winter. On the other hand, coastal area of Portugal and Galicia has similar characteristic of SST variability with the north part of the open sea during summer and with the west part of the open ocean during winter. This implies that the Biscay bay has high summer SST, which is more or less similar to the Mediterranean Sea, and cold winter SST compared to the coastal area of Portugal

4.2.2 Temporal variation

Figure 14 illustrate the loadings of PC1 of the SEA. The loadings graph begins in January 1, 1982, where the loading is negative. In general, for each year, January, February, March and December has a negative loadings and June, July, August and September has a positive loadings. We can learn two things from the loadings from the PC1, first, the loadings show that there are seasonal variations throughout the time series. During summer, there is a positive loadings and in winter negative loadings. Second, the positive peaks of loadings are not the same for each season. These high positive and low negative loadings indicate that, these particular months of the years had the highest summer temperature and lowest winter temperature respectively in the study area.
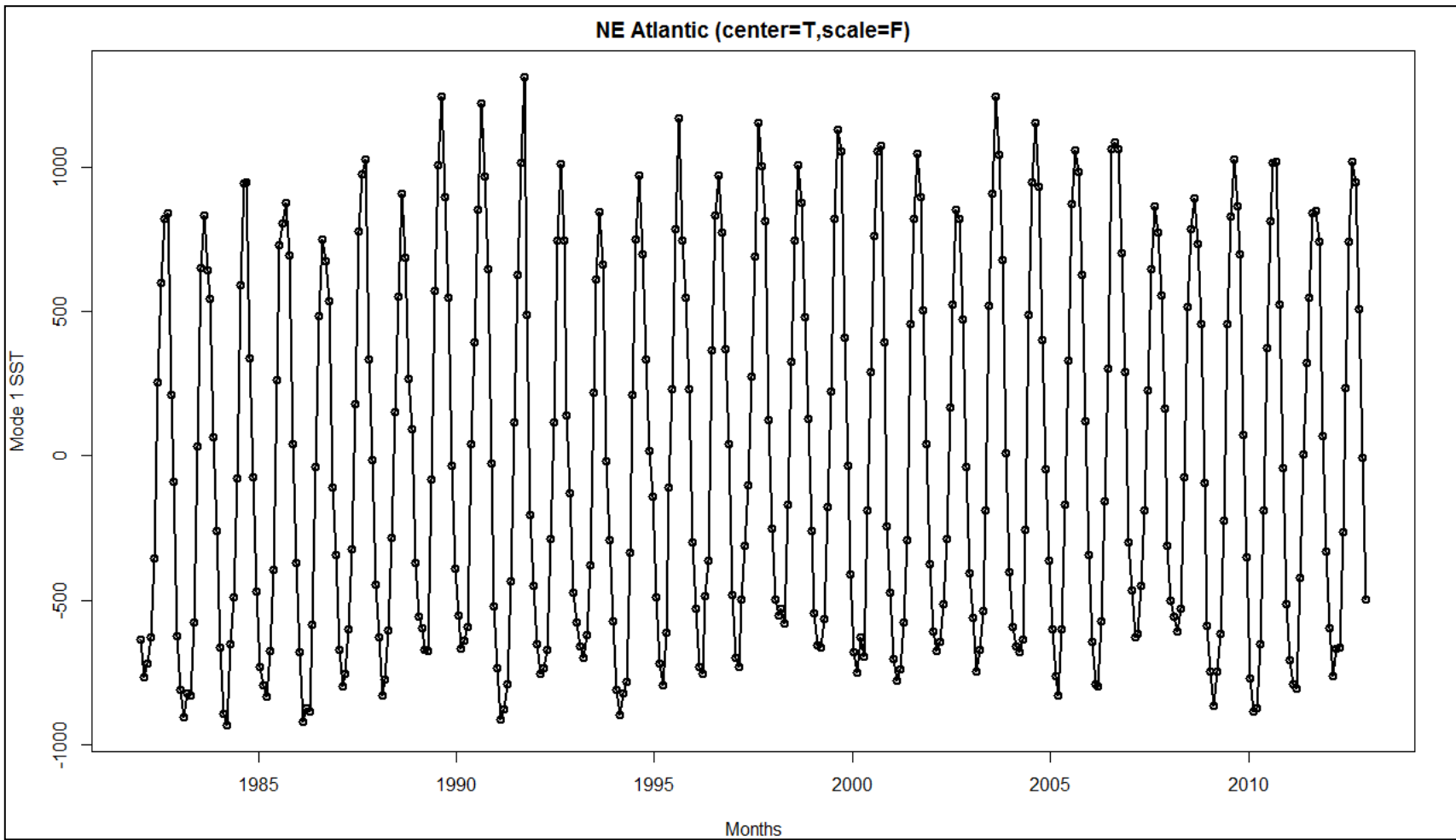
Figure 14. Loadings of PC1.

Figure 15 and 16 shows the seasonal variation of SST in SEA. Even if each year was similar to the other years, there were some seasonal differences as indicated by the graphs. During summer, September 1991 has the highest positive loading followed by August of 2003 and 1989. Year 2006 has the same loadings during summer (June, July and August). On the other hand, Figure 16 shows during winter (December, January and February) year 1982 has the highest negative loadings followed by 1993 and 2008. Moreover, 1986 has the highest negative loadings during March, April and May.
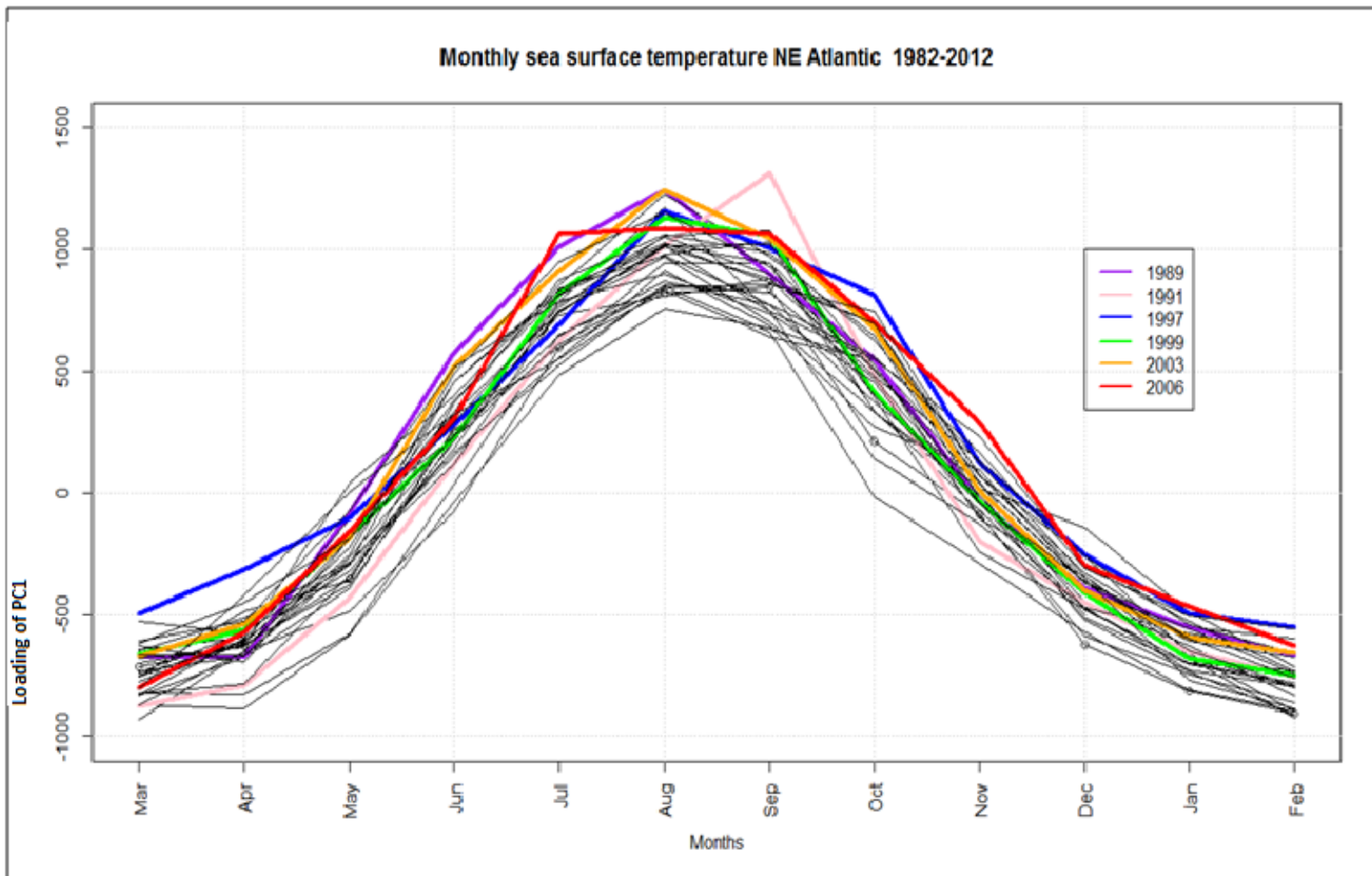
Figure 15. Loadings of PC 1 of SEA from year 1982 to 2012 showing the highest positive loadings in colors.
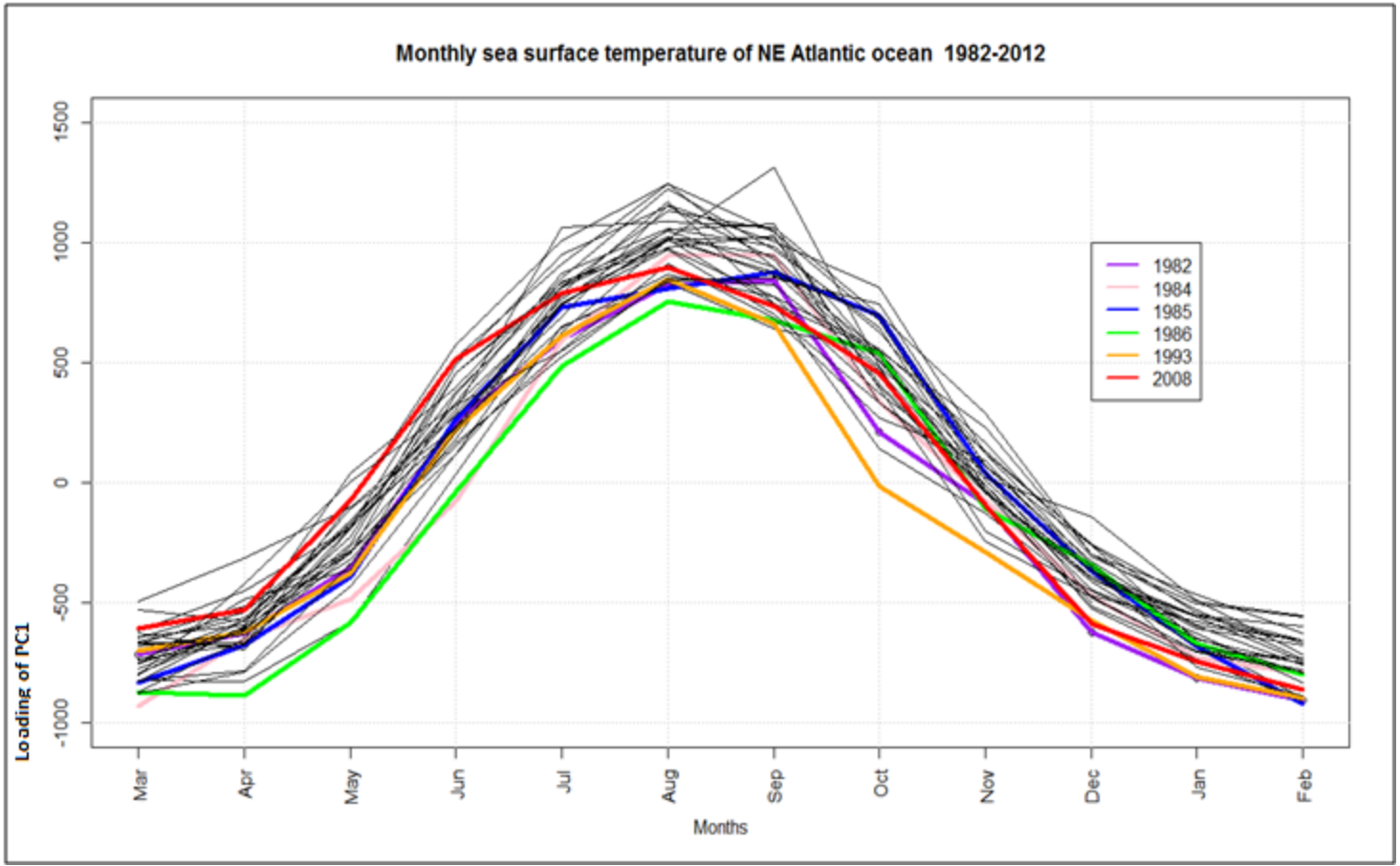
Figure 16. Loadings of PC 1 of SEA from year 1982 to 2012 showing the highest negative loadings in colors.

5. Discussion

In this study, Pathfinder V5 and MODIS SST images were analyzed by EOF to extract the variability of SST over the Northern Iberia Shelf. The analysis revealed that there exists a strong spatial and temporal variation of SST in the study area. The temporal pattern at the NIS was dominated by a strong seasonal variability which was also observed at a larger scale in the Southeastern European Atlantic (SEA). In the NIS, the higher SST are generally observed in August and the lower SST from January to March. At the larger scale (SEA), the seasonal pattern is very similar although there are differences in the maximum and minimum seasonal SST that are related with the latitudinal gradient of the area. We may conclude that the SST seasonal pattern is related with the general climatic characteristics of this mid-latitude area.

Within the NIS, however, the strong gradient of the PC1 scores revealed differences in the amplitude of the seasonal signal. PC1 scores were always positive. Therefore, higher and lower spatial scores revealed higher or lower amplitudes of the seasonal signal respectively. In the Galician shelf, where the lowest PC1 scores were observed, SST oscillates between a summer maximum mean of c. 18 ºC and a winter minimum mean of c. 13 ºC (Annex 1). The PC1 scores increases, the amplitude of the signal is progressively amplified along the coast towards the inner Bay of Biscay where summer maximum SST is >20 ºC and winter minimum is <13 ºC. This difference in the amplitude is the consequence of two hydrodynamic processes. At the western Iberian Shelf, the northward displacement and intensification of the Azores High during summer and the development of thermal lows over the Iberian Peninsula favors equatorward winds that provoke intense and frequent coastal upwelling and associated filaments, and induce the ascent up to the surface of sub-surface cold, nutrient-rich waters along the northwest (Pingree, & Le Cann, 1992b). Coastal upwelling occurs between March and October, with maximum intensity during the summer. This process is the reason why the western Iberia near Galician cost

exhibit relatively low SST during summer. Further, the intensity of coastal upwelling decreases along the Cantabrian shelf towards the inner Bay of Biscay, where its influence is minimum or negligible. On the contrary, at the inner Bay of Biscay, the shape of the Bay favors stagnation of surface water masses, with the consequent enhancement of surface thermal stratification. This stagnation process therefore contributes to reinforce the SST alongshore gradient caused by the intensity of coastal upwelling in the area. In winter, however, the seasonal SST gradient was reversed, although much less apparent. Hence, the winter SST spatial pattern also contributes to the spatial gradient of the amplitude of the seasonal signal. The western Iberian Shelf exhibits higher SST that decreases eastward along the Cantabrian shelf, with the lowest SST occurring at the inner Bay of Biscay. By the end of the summer a subsurface slope current, named the Iberian Poleward Current (IPC), starts to develop and transports warm (and salty) Eastern North Atlantic Central Water of sub-tropical origin (ENACWT) towards the North along the Western Iberian shelf (Frouin et al., 1990). This current is favored by the reversal of northerly winds during the summer to southerlies or southwesterlies in Autumn. Between December and March, it surfaces, rounds Cape Finisterre, and proceeds along the shelf edge and upper slope off Northern Iberia Shelf break , penetrating into the inner Bay of Biscay along the Cantabrian coast with decreasing intensity (Pingree and Le Cann, 1990).. Thus, IPC is the most probably the main reason behind the inverse SST variability observed in the study area during winter, although its intensity varies between years.Also in winter, the influence of the Adour river decreases SST at the inner shelf and contributes to the summer-opposed gradient of SST.

Our study also showed that besides the geographical differences in the amplitude of the seasonal SST signal, there were also inter-annual differences in the amplitude, the timing of the maxima and minima, or in general at any particular time of the period of study. The latter occurs both at the large scale of the SEA and at the NIS. For instance, at the large scale of the SEA September 1991 was the highest SST followed by August 2003 and 1989 in our time series 1982 to

2012, whereas August 2003 was the highest SST followed by September 1991 and July 2006 in NIS.

With our preliminary analysis we identified periods that present particular higher-than-average and lower-than-average SST, and the comparison between both spatial scales allowed us to hypothesize if this variability is the consequence of large scale climatic variability or of mesoscale hydrodynamic processes. For instance, lower than average PC1 scores in winter both at the large scale (SEA) and in the NIS could be related with cold and/or with frequent strong storms conditions that would favor vertical mixing and reducing SST and that are in general controlled by large scale climatic processes (e.g. the North Atlantic Oscillation; Barnston & Livezey, 1987). Alternatively, relatively higher winter SST in the NIS compared to the SEA would reflect a year of higher intensity of the IPC. This was the case of the autumn-winter 2006-2007, when Le Cann & Serpette (2009) identified a particularly strong IPC. During the summer, higher than average SST values both at the large scale (SEA) and in the NIS could be related with warmer than average large scale climatic conditions, whereas colder than average SST in the NIS compared to the SEA would reflect higher intensity in coastal upwelling.

The seasonal STT variation has important consequences on the characteristics and dynamics of the marine ecosystem, for instance, on primary production and on the general productivity of the ecosystem that sustains important fisheries. The EOF analysis carried out in this study, which allowed representing more than 90% of SST variability in the area with a single mode, will help to understand the processes that may provoke changes on the NIS ecosystem.

6. Conclusion

The time series analysis of Satellite derived SST data revealed the spatial pattern, timing and relative magnitude of seasonal and interannual SST variation in the study area. The use of the EOF proved to be a useful method for describing the seasonal and temporal SST pattern in the study area. The study shows that there was a clear cyclic pattern and this cyclic pattern was heterogeneous in the study area.

In general from the temporal pattern we can conclude that the higher SST was observed during August and the lower SST from January to March in the study area. Moreover, this pattern is variable, spatially and in magnitude from year to year.

From the spatial pattern we can conclude that there were differences in the amplitude of seasonal signal, were higher amplitude signals are more to related to the inner Bay of Biscay and lower amplitude signals were related to the western Iberia near Galician cost. This variation was due to the costal upwelling and the variation of IPC intensity from year to year.

The comparison between the NIS and SEA allowed us to see the similarity and the difference variability of seasonal SST variation exhibited by the NIS from the larger scale of SEA and helped us to hypothesize the possible reasons for this variation.

Finally, we conclude that the main mesoscale processes, vertical mixing in winter, stratification in summer and IPC were the main reason behind on the spatial differences in the seasonal signal and the interannual variability of SSTin the study.

References

Bardey, P., Garnesson, P., Moussu, G., and Wald, L., (1999). *Joint analysis of temperature and ocean colour satellite images for mesoscale activities in the Gulf of Biscay*. International Journal of Remote Sensing, 20: 1329-1341.

Barnston, A. G., and R. E. Livezey, 1987: *Classification, seasonality and persistence of low-frequency atmospheric circulation patterns*. Mon. Wea. Rev., **115**, 1083-1126.

Barton, E. D. (1998). *Eastern boundary of the North Atlantic: Northwest Africa and Iberia coastal segment*. In The Sea (Ed. by A. R. Robinson and K. H. Brink). Pp. 633–658. John Wiley & Sons, Inc.

Bernard Le Cann , Alain Serpette. (2009). *Intense warm and saline upper ocean inflow in the southern Bay of Biscay in autumn–winter 2006–2007*. Continental Shelf Research, 29. pp 1014–1025

Blanchard, F., and Vandermeirsch, F. (2005). *Warming and exponential abundance increase of the subtropical fish Capros aper in the Bay of Biscay (1973–2002)*. Comptes-rendus de l'académie des sciences, 328: 505–509.

Botas JA, Fernández E., Bode A., and Anadón R., (1990*). A persistant upwelling off the Central Cantabrian Coast (Bay of Biscay)*. Estuarine, Coastal and Shelf Science 30: 185-199.

Brander, K. M., Blom, G., Borges, M. F., Erzini, K., Hendersen, G., MacKenzie, B. R., Mendes, H., Santos, A. M. P., and Toresen, R. (2003). *Changes in fish distribution in the Eastern North Atlantic; are we seeing a coherent response to changing temperature?* ICES Marine Science Symposia, 219: 261–270.

Cabal J., González-Nuevo G., Nogueira E. 2008. *Mesozooplankton species distribution in the NW and N Iberian shelf during spring 2004: Relationship with frontal structures.* Journal of Marine Systems 72, 282-297.

Emry, W.E. & Thomson, R.E. (1997) *Data Analysis Methods in Physical Oceanography*. Pergamon. Oxford, New York, Tokyo.

Eastman, J.R., & Fulk, M. (1993) *Long Sequence Time Series Evaluation using Standardized Principal Components*. Photogrammetric Engineering and Remote Sensing 59: 1307-1312.

Fernández E, Bode A (1991) *Seasonal patterns of primary production in the Central Cantabrian Sea (Bay of Biscay).* Scientia Marina 55: 629-636

Fernández E, Cabal J, Acuña JL, Bode A, Botas A, García-Soto C (1993) *Plankton distribution across a slope current-induced front in the southern Bay of Biscay.* Journal of Plankton Research 15: 619-641.

Frouin, R., A. F., Fuiza, I. Ambar, and T. J., Boyd (1990), *Observations of a Poleward Surface Current off the coasts of Portugal and Spain during the winter.* Journal of Geophysical Research, 95(C1), 679-691

Galladudet, T.C. and Simpson, J.J., (1994) *"An Empirical Orthogonal Function Analysis of Remotely Sensed Sea Surface Temperature Variability and its Relation to Interior Oceanic Processes off Baja California,"* Remote sens. Environ., Vol. 47, pp. 375-389.

Garcia-Soto, C., (2004). *'Prestige' oil spill and Navidad flow.* Journal of the Marine Biological Association of the United Kingdom 84, 297–300.

Garcia-Soto, C., Pingree, R.D., Valde´ s, L., (2002). *Navidad development in the southern Bay of Biscay: climate change and swoddy structure from remote sensing and in situ measurements*. Journal of Geophysical Research 107 (C8).

Haynes, R., and Barton, E. D. (1990). *A poleward flow along the Atlantic coast of the Iberian Peninsula*. Journal of Geophysical Research, 95: 11425–11441.

Jensen, J.R. (2005) *Introductory Digital Image Processing. A Remote Sensing Perspective*. Prentice Hall.

Keiner, L.E. and Yan, X.H., (1997) *"Empirical Orthogonal Function Analysis of Sea Surface Temperature Patterns in Delaware Bay,"* IEEE Transactions on Geoscience and remote sensing, Vol. 35, No. 5, pp. 1299-1306.

Kilpatrick, K.A., G.P. Podesta and R. Evans. 2001. *Overview of the NOAA/NASA Advanced Very High Resolution Radiometer Pathfinder algorithm for sea surface temperature and associated matchup database.* J. Geophys. Res.-Oceans, 106 (C5): 9179-9197.

Koutsikopoulos, C. and LeCann, B.(1996) *Physical processes and hydrological structures related to the Bay of Biscay anchovy.* Sci. Mar. 60, 9–19,.

Lagerloef, G.S.E. and Bernstein, R.L., (1988). *"Empirical Orthogonal Function Analysis of Advanced Very High Resolution Radiometer Surface Temperature Patterns in Santa Barbara Channel,"* J. Geo. Res., Vol. 93, No. C6, pp. 6863-6873.

Lavin, A., Valdes, L., Sanchez, F., Abaunza, P., Forest, J., Boucher, P., Lazure, P., and Jegou, A. M. (2005). *The Bay of Biscay: The encountering of the ocean and the shelf. In The Global Coastal Ocean: Interdisciplinary Regional Studies and Syntheses.* The Sea, vol. 14. (Ed. by A. R. Robinson and K. H. Brink). Pages 933–1001. Harvard Press.

Legendre L, Rassoulzadegan F (1996) *Food-web mediated export of biogenic carbon in oceans: hydrodynamic control.* Mar Ecol Prog Ser 145:179–193

Lillesand, M. and Kiefer, R.W. (1999). Remote sensing and image interpretation. Fourth edition. John Willy & Sons Inc. Newark, Chichester, Wenheim, Brisbane, Singapore, Toronto. 595 pp.

Llope M, Anadón R, Viesca L, Quevedo M, González-Quirós R, Stenseth NC (2006) *Hydrography of the southern Bay of Biscay shelf-break region: Integrating the multiscale physical variability over the period 1993–2003.* Journal of Geophysical Research 111: C09021.

Mann K.H., Lazier J.R.N. (1996). *Dynamics of Marine Ecosystems*. Blackwell Science Inc.

Nogueira & González-Quirós (2011) *case study: North Western Iberia (NWI) sub-region.*

OSPAR. 2000. Quality Status Report 2000. *Region IV _ Bay of Biscay and Iberian coast.*

Paden, C.A., Abbott, M.R., and Winant, C.D. (1991*). "Tidal and Atmospheric Forcing of the Upper Ocean in the Gulf of California, 1: Sea Surface Temperature Variability,"* J. Geophys. Res., Vol. 96, No. C10, pp. 18337-18359.

Pauly, D., and Christensen, V. (1995) *Primary production required to sustain global fisheries.* Nature 374: 255-257.

Peliz, A., Dubert, J., Santos, A. M. P., Oliveira, P. B., and Le Cann, B. (2005). *Winter upper ocean circulation in the Western Iberian Basin - Fronts, Eddies and Poleward Flows: an overview,* Deep-Sea Research Part I Oceanographic Research Papers, 52(4): 621–646.

Pingree, R. D. and Le Cann, B. (1989). *Celtic and Armorican slope and shelf residual currents, Progr.* Oceanogr., 23, 303–338.

Pingree, R. D. and Le Cann, B.(1990).*Structure, strength and seasonality of the slope currents in the Bay of Biscay region*, J. Mar. Biol. Assoc. UK, 70, 857–885.

Pingree, R.D., Le Cann, B., 1992b. *Three anticyclonic slope water Oceanic eDDIES (SWODDIES) in the Southern Bay of Biscay.* Deep Sea Research I 39, 1147–1175.

Pingree, R. (1993). *Flow of surface waters to the west of the British Isles and in the Bay of Biscay,* Deep-Sea Res. Pt. II, 40, pp.369–388.

Prego, R and Vergara, A R (1989) *Nutrient fluxes to the Bay of Biscay from Cantabrian rivers (Spain)* Oceanologica Acta 21: 271-278.

R Development Core Team (2009). *R: A language and environment for statistical computing*. Vienna, Austria: R Foundation for Statistical Computing.
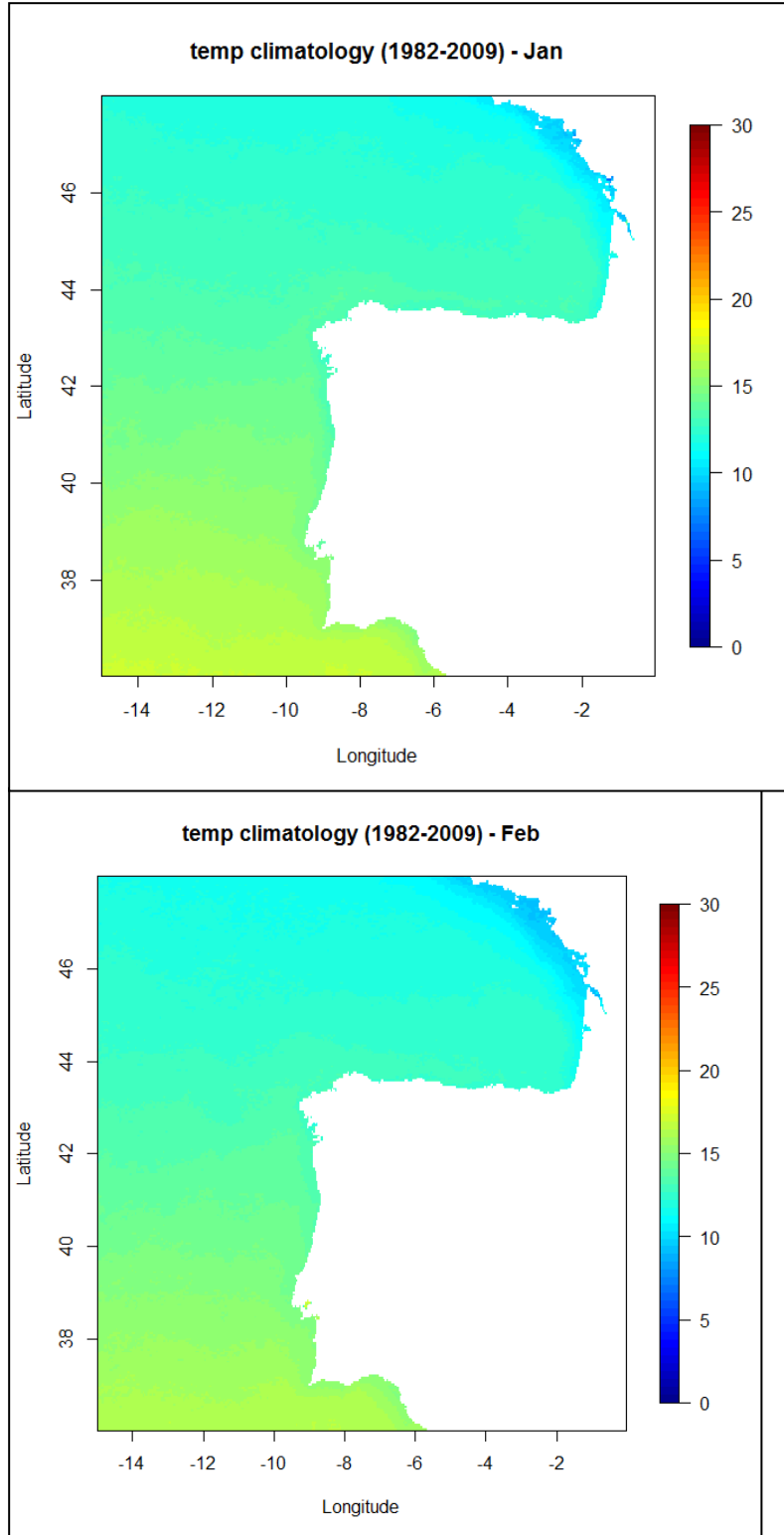
Tarumay G., Sudip J., & Arun S. (2014). *"Implication of Empirical Orthogonal Function analysis to objectively analyzed sea surface temperature data of Bay of Bengal.* Indian Journal of Geo-Marine science. Vol.43, pp. 39-44.
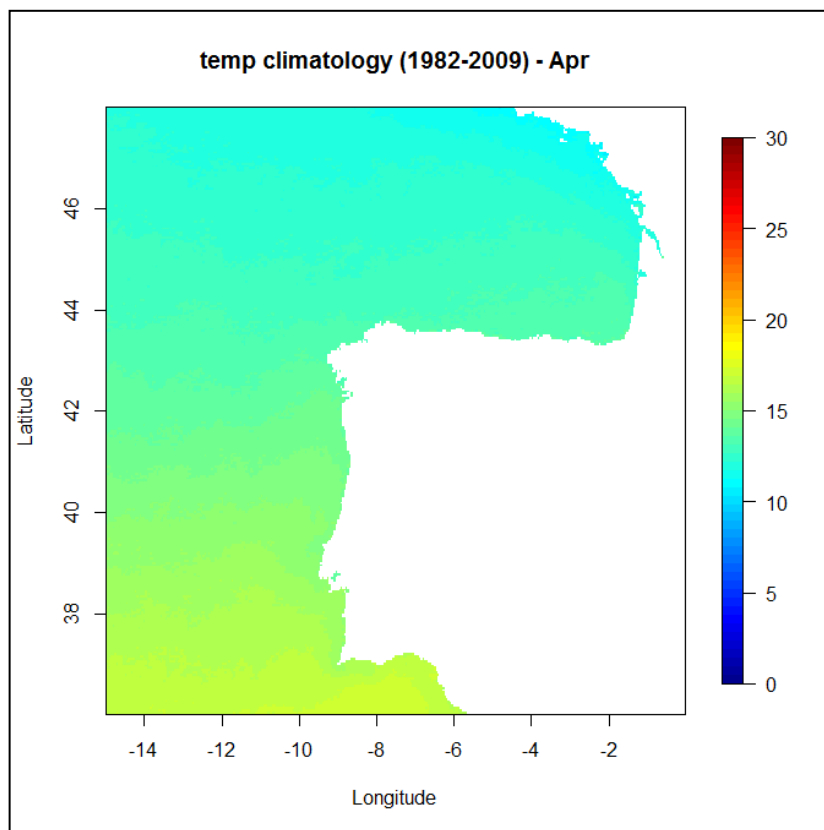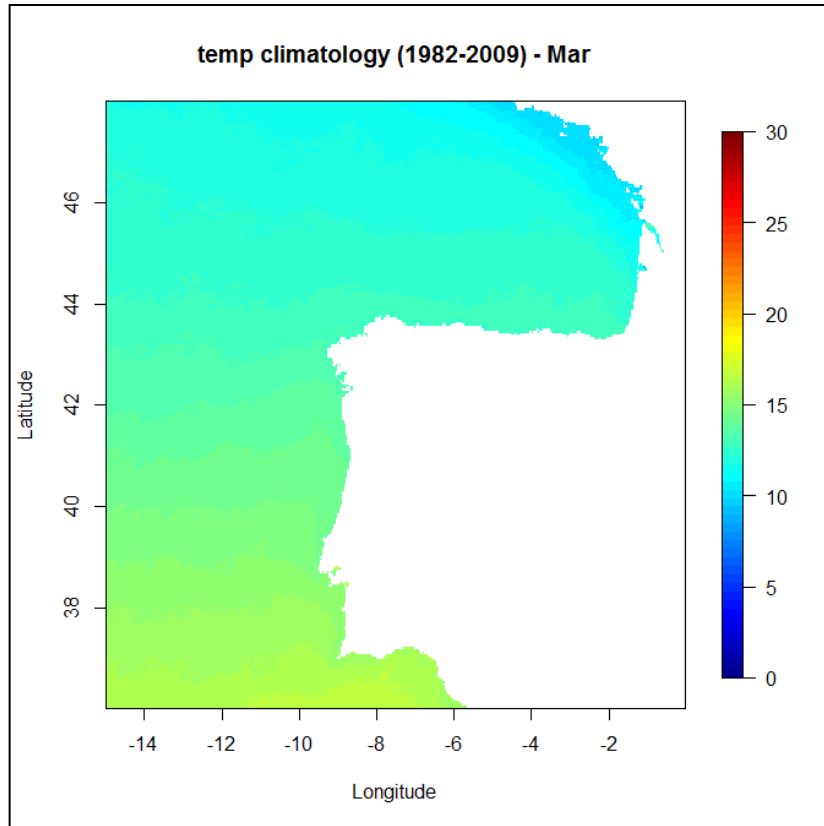
Walton C. C., W. G. Pichel, J. F. Sapper, D. A. May. (1998). *The development and operational application of nonlinear algorithms for the measurement of sea surface temperatures with the NOAA polar-orbiting environmental satellites*, J. Geophys. Res., 103: (C12), 27999-28012.

Yoder, J.A., Schollaert, S.E. & O'Reilly, J.E. (2002) *Climatological phytoplankton chlorophyll and sea surface temperature patterns in continental shelf and slope waters off the northeast U.S. coast*. Limnology and Oceanography 47. No.3, 672-682.
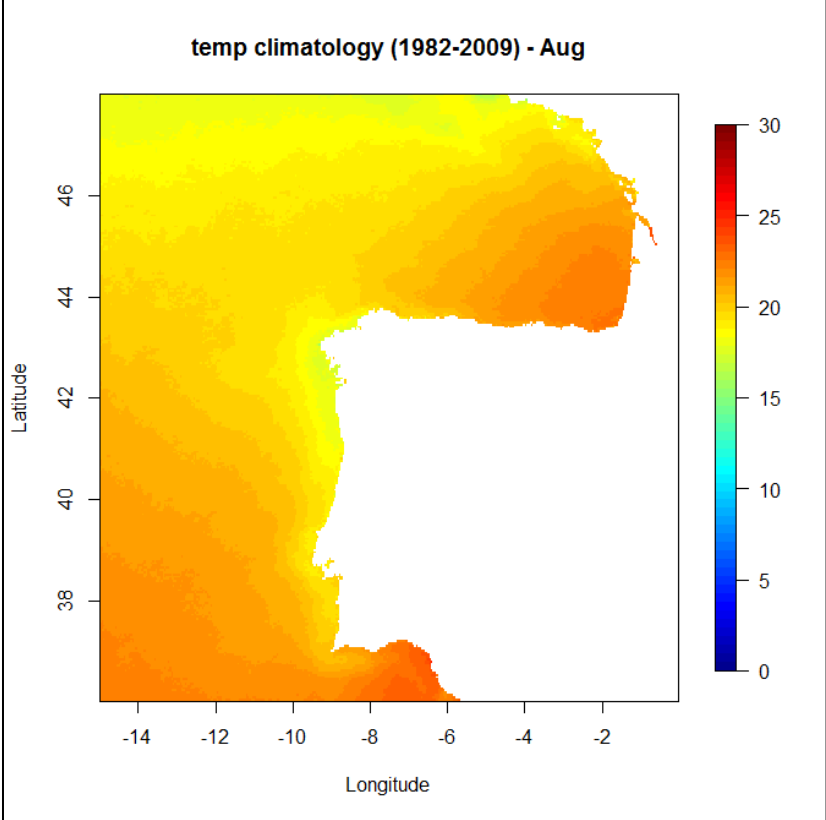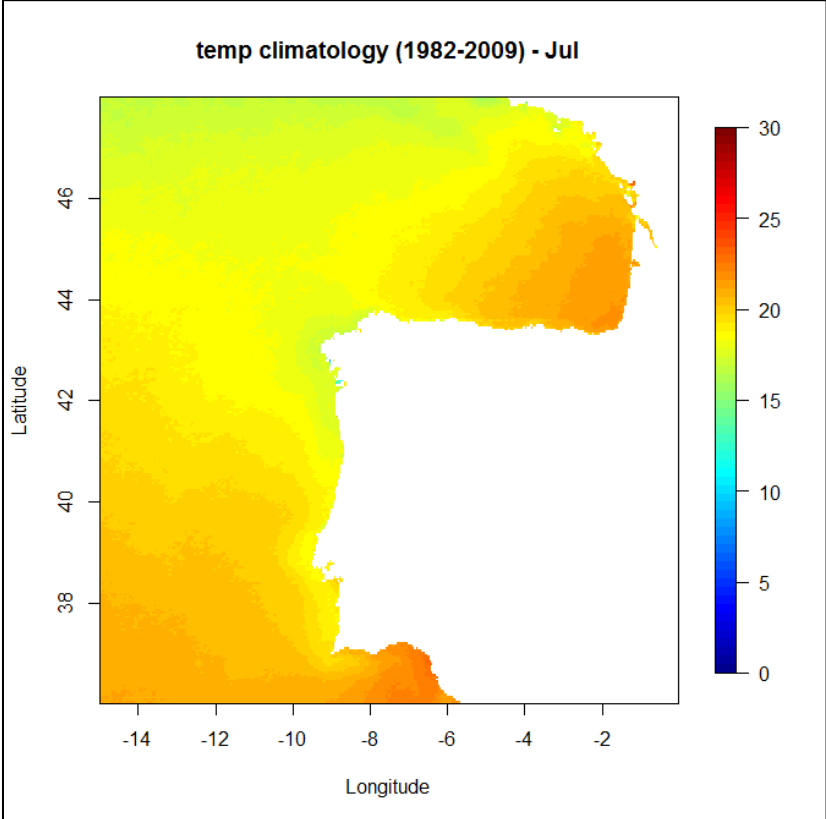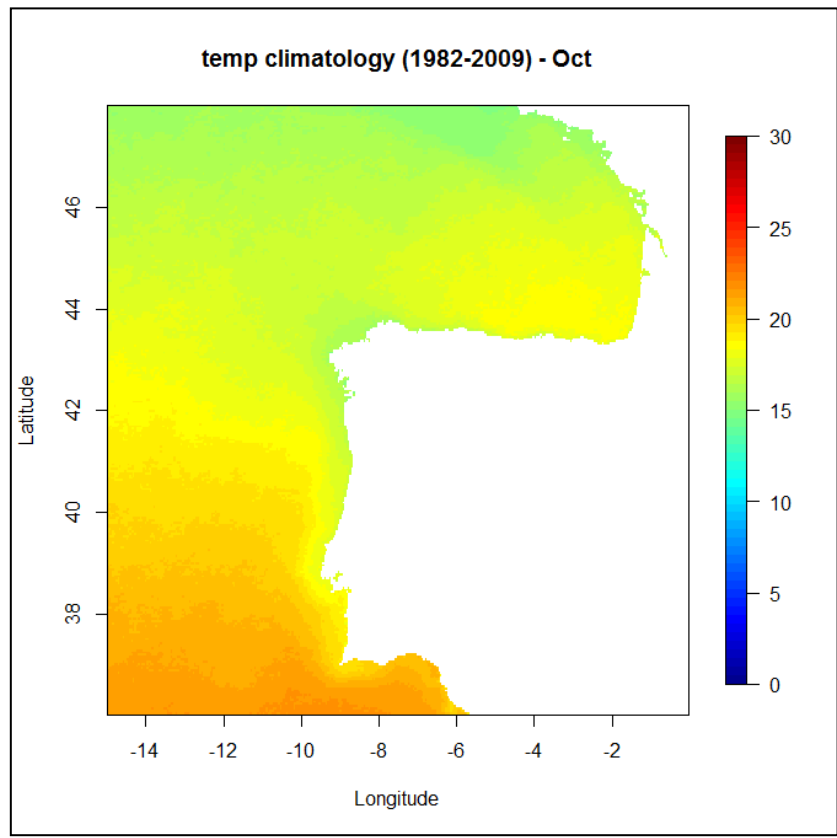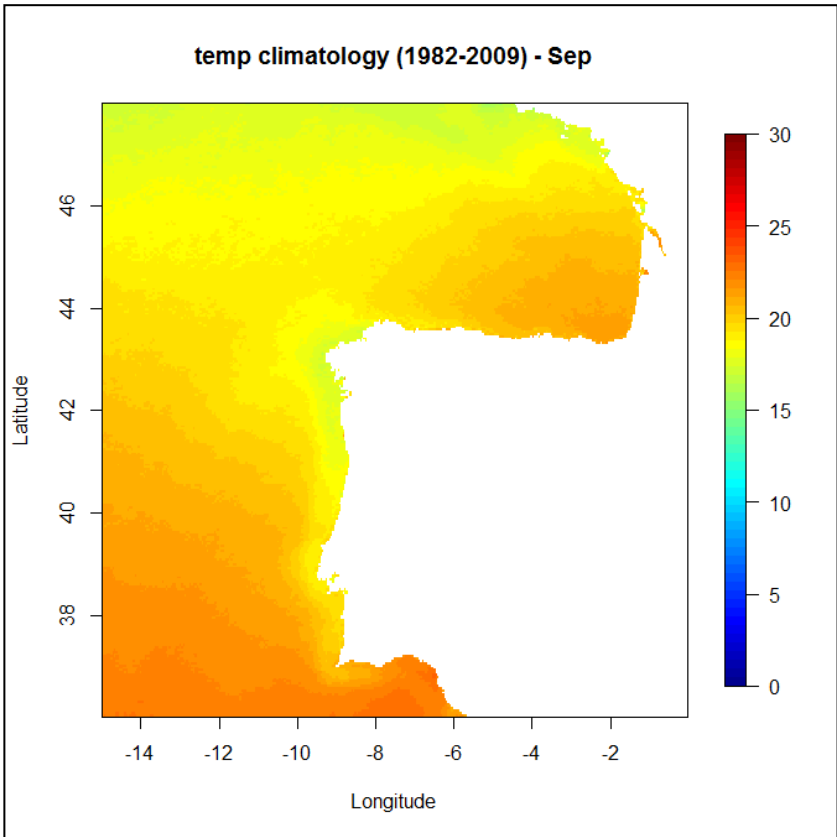
ANNEX

1.1. Seasonal SST (in degree centigrade) Climatology of Pathfinder 1982 -2009

temp climatology (1982-2009) - Mar

temp climatology (1982-2009) - Apr

temp climatology (1982-2009) - May

temp climatology (1982-2009) - Jun

temp climatology (1982-2009) - Jul

temp climatology (1982-2009) - Aug

temp climatology (1982-2009) - Sep

temp climatology (1982-2009) - Oct

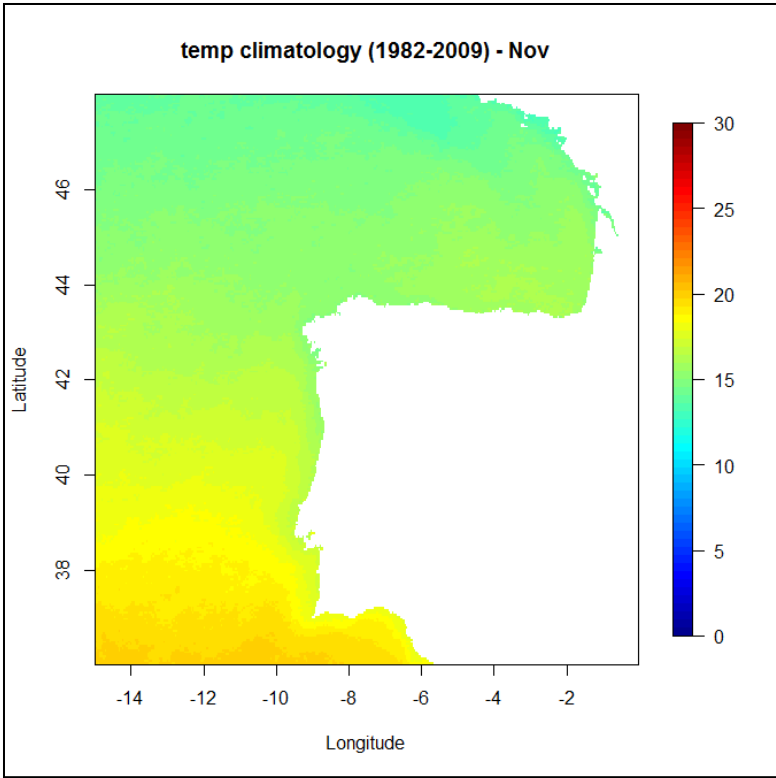temp climatology (1982-2009) - Nov
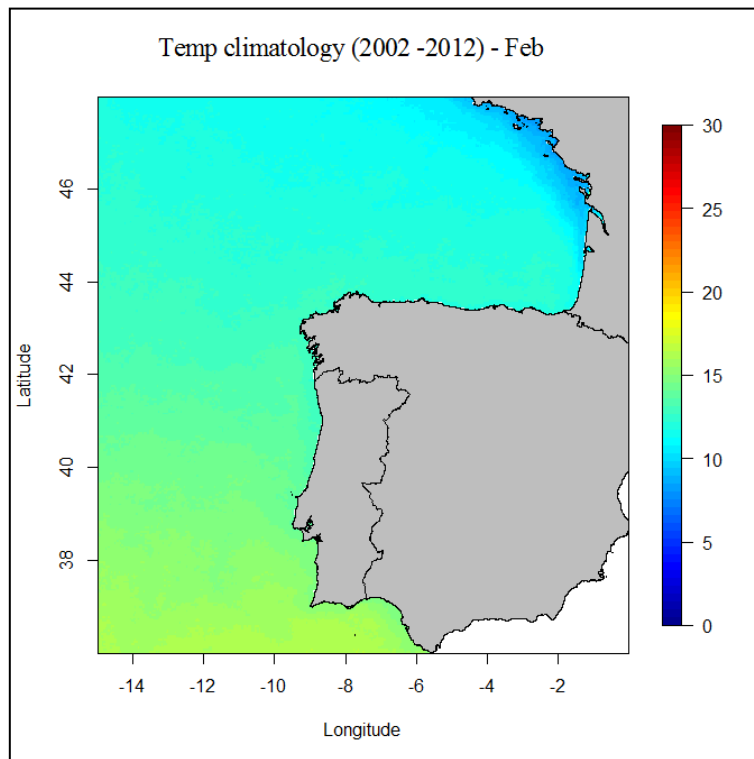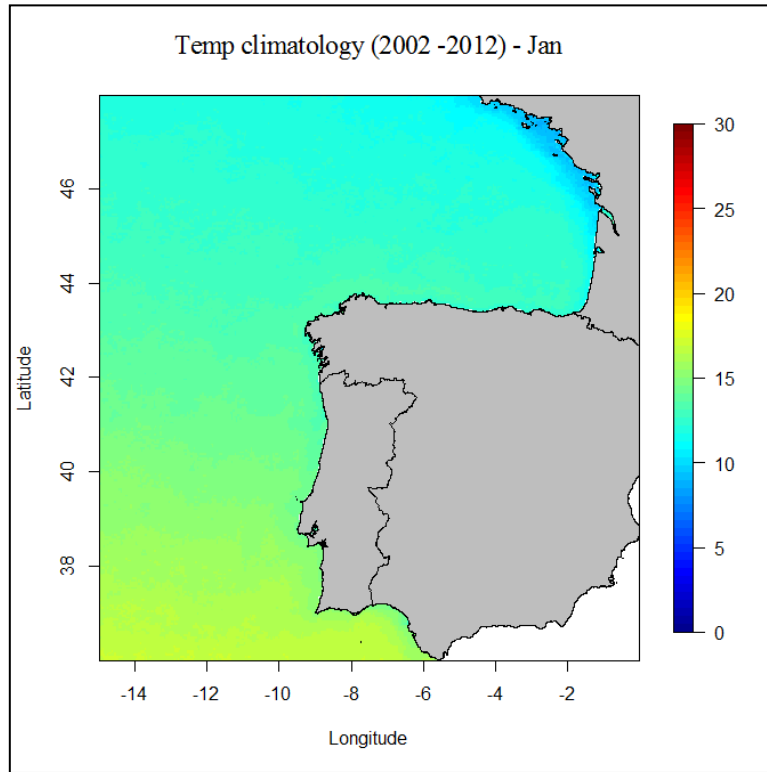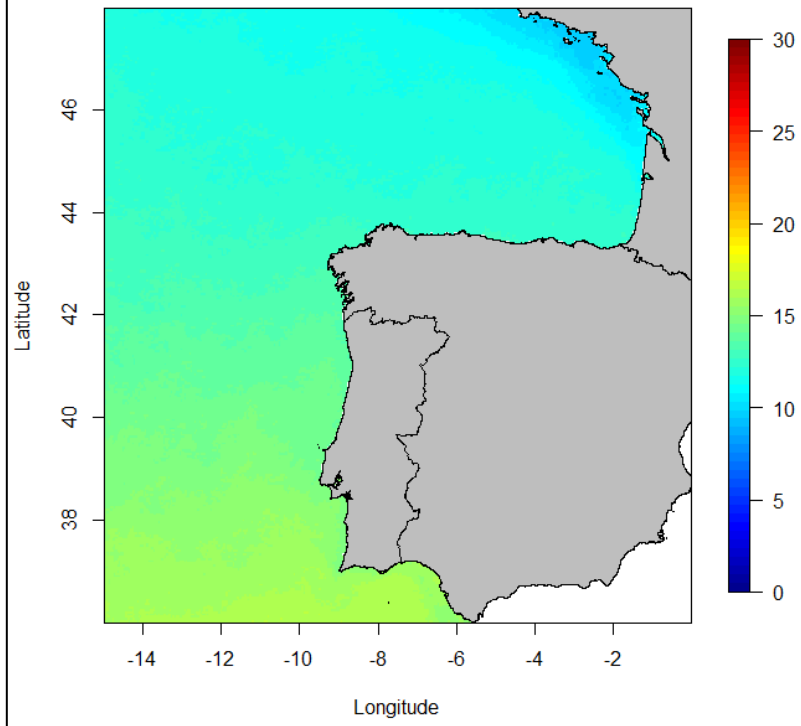

temp climatology (1982-2009) - Dec
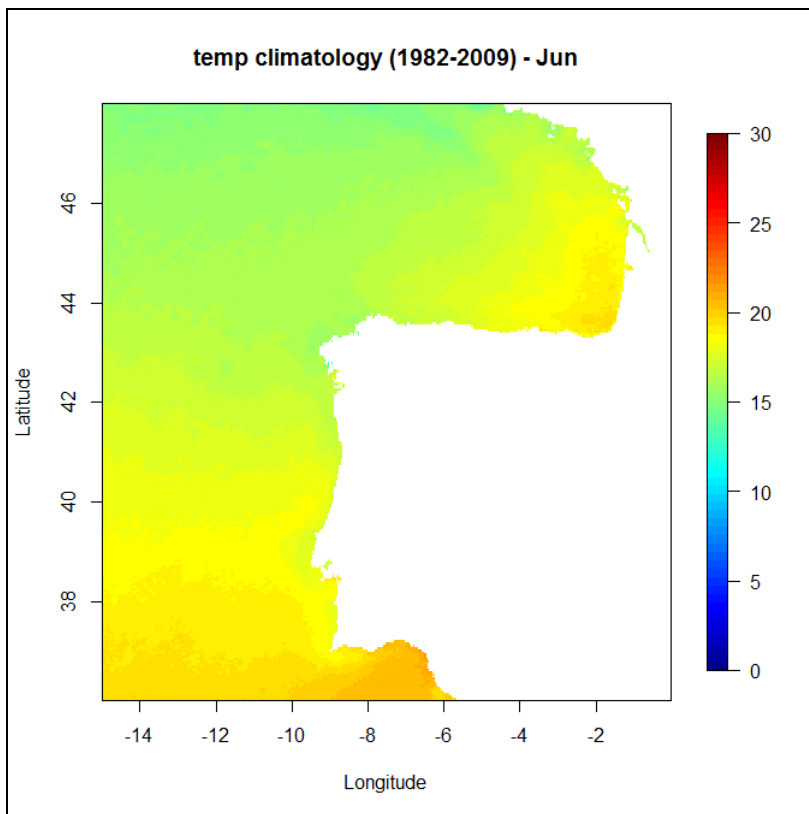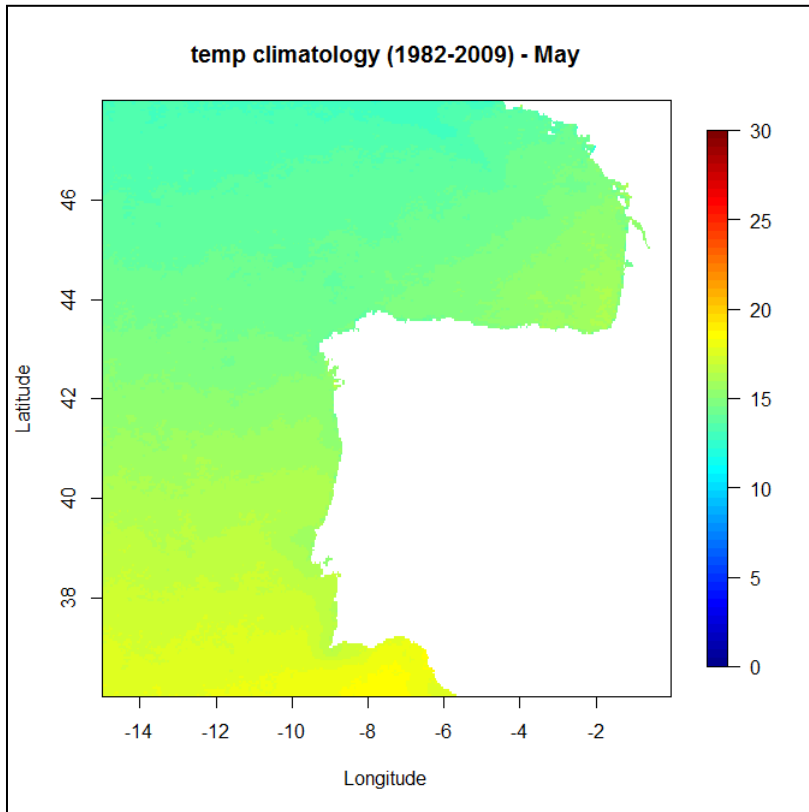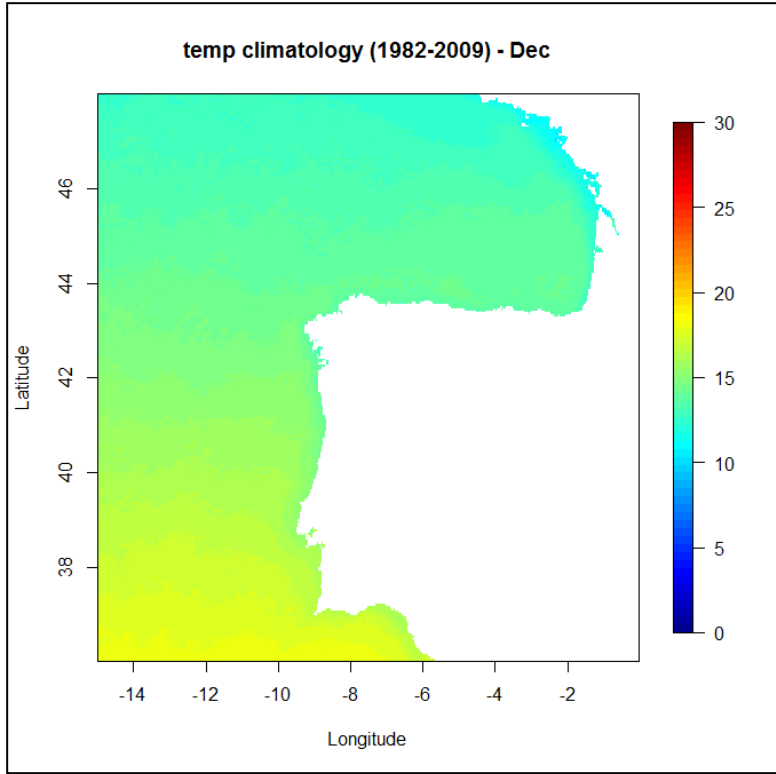
1.2 . Seasonal SST (in degree centigrade) Climatology of MODIS 2002 -2012

Temp climatology (2002 -2012) - Jan

Temp climatology (2002 -2012) - Feb

Temp climatology (2002 -2012) - Mar

Temp climatology (2002 -2012) –Apr

Temp climatology (2002 -2012) - May

Temp climatology (2002 -2012) - Jun

Temp climatology (2002 -2012) –Jul

Temp climatology (2002 -2012) –Aug

Temp climatology (2002 -2012) –Sep

Temp climatology (2002 _2012) - Oct

Temp climatology (2002 _2012) - Nov

Temp climatology (2002 _2012) - Dec